

Deep structure of the Demerara Plateau and its two-fold tectonic evolution: from a volcanic margin to a Transform Marginal Plateau, insights from the conjugate Guinea Plateau

Graindorge David ¹, Museur Thomas ^{1,2}, Klingelhoef Frauke ², Roest Walter ², Basile C. ³, Loncke L. ⁴, Sapin F. ⁵, Heuret A. ⁶, Perrot Julie ¹, Marcaillou B. ⁷, Lebrun J-F ⁸, Déverchère Jacques ¹

¹ University of Brest, CNRS, IUEM, Plouzané, France

² Ifremer, Centre de Brest, UR Géosciences Marines, BP 70, 29280 Plouzané, France

³ ISTerre, UMR-CNRS 5275, Observatoire des Sciences de l'Univers de Grenoble, Université Joseph Fourier, Maison des Géosciences, 1381 rue de la Piscine, 38400 St. Martin d'Hères, France

⁴ University of Perpignan Via Domitia, Centre de Formation et de Recherche sur les Environnements Méditerranéens (CEFREM), UMR 5110, 52 Avenue Paul Alduy, 66100, Perpignan, France

⁵ Total SA, Centre Scientifique et Technique Jean Feger (CSTJF), Avenue Larribau, 64018, Pau, France

⁶ Université de Guyane, Géosciences Montpellier, Université de Montpellier, CNRS Université des Antilles, Cayenne, Guyane

⁷ University Côte d'Azur, CNRS, Observatoire de la Côte d'Azur, IRD, Géoazur, Valbonne, France

⁸ Géosciences Montpellier, Université de Montpellier, CNRS, Université des Antilles, Pointe à Pitre, Guadeloupe (FWI)

Abstract :

Transform marginal Plateaus (TMPs) are large and flat structures commonly found in deep oceanic domains, but origin and relationship to adjacent oceanic lithosphere remain poorly understood. This paper focuses on two conjugate TMPs, the Demerara Plateau off Suriname and French Guiana and the Guinea Plateau, located at the junction of the Jurassic Central Atlantic and the Cretaceous Equatorial Atlantic Oceans. The study helps to understand (1) the tectonic history of both Demerara and Guinea Plateaus, (2) the relationship between the Demerara Plateau and the adjacent oceanic domains and finally, (3) to throw light on the formation of Transform Marginal Plateaus (TMPs). We analyze two existing wide-angle seismic derived velocity models from the MARGATS seismic experiment (Demerara Plateau), and adjacent composite industrial seismic lines covering the Demerara and Guinea Plateaus. The Demerara Plateau displays a 30 km thick crust, subdivided into 3 layers, including a high velocity lower crust (HVLC). The velocities and velocity gradients do not fit values of typical continental crust but instead correspond to volcanic margin or Large Igneous Province (LIP) type crusts. We propose that the, possibly continental, lower crust is intruded by magmatic material and that the upper crustal layer is made of extrusive volcanic rocks of the same magmatic origin, forming thick seaward (westward) dipping reflectors (SDRs) sequences. This SDR complex extends to the Guinea Plateau as well and was emplaced during hotspot

(Sierra Leone)-related volcanic rifting preceding the Jurassic opening of the Central Atlantic and forming the western margin of the plateau. N-S composite lines linking Demerara and Guinea plateaus reveal the spatial extent of the SDR complex but also a preexisting basement ridge separating the two plateaus. The entire Demerara-Guinea margin would therefore be an inherited Jurassic volcanic margin bordering the Central Atlantic Ocean to the east, with as a possible conjugate being the Bahamas Plateau on the other side of the ocean. This margin was then reworked during a non-coaxial Cretaceous second phase of rifting potentially accompanied by a magmatic event. Opening of the northern margin occurs in a transform mode splitting the Jurassic volcanic margin in two parts (Guinea and Demerara TMPs), conceivably along a pre-existing basement ridge. Rifting of the eastern part of the Demerara Plateau occurred surprisingly along the eastern limit of the Jurassic SDR complex, forming the present-day eastern divergent margin of the Demerara Plateau. After that stage, the Demerara and Guinea plateaus are individualized on each side of the Equatorial Atlantic. This study also highlights the major contribution of thermal anomalies related to hotspots and superposed tectonic phases in the case of other TMPs which share numerous characteristics with the Demerara Plateau.

52 **Introduction**

53 Marginal plateaus have been recognized as submarine seafloor highs with a flat (or
54 sub-horizontal) top and located clearly deeper than the standard shelf break within the
55 continental slope (Mercier de Lépinay et al., 2016). Most of them are located at the
56 junction between two oceanic domains of different ages (Mercier de Lépinay et al., 2016).
57 For those bordered by at least one transform or oblique margin, Loncke et al. (2020)
58 define the sub-category of Transform Marginal Plateaus (TMPs). As most of these plateaus
59 are associated with at least one major magmatic event (Loncke et al., 2020), TMPs have
60 possibly recorded polyphase tectonic and magmatic histories. Therefore, they provide
61 geodynamic records that may help to better understand complex ocean opening
62 processes, break-up conditions, and the thermomechanical evolution of continental
63 margins at the junction between divergent and transform margins.

64 Located on each side of the Equatorial Atlantic, the Demerara and Guinea Plateaus
65 are both TMPs corresponding to conjugated transform margins. The Demerara/Guinea
66 TMPs formed at the southern tip of the Jurassic Central Atlantic Ocean and later separated
67 and individualized in a transform mode during the highly oblique Cretaceous (Aptian-
68 Albian) Equatorial Atlantic gateway opening (Nemčok et al., 2015). Different spreading
69 vectors of the Central and Equatorial Atlantics required a development of the
70 Accommodation Block, its role was to accommodate for about 20° mismatch between the
71 Central and Equatorial Atlantic spreading vectors, which decreased from late Aptian-
72 Albian to Paleocene down to 0° (Nemčok et al., 2015).

73 Across the Demerara Plateau (Figure 1), several academic and industrial data sets
74 have been acquired over the past 20 years which makes it one of the most imaged TMPs.
75 Even if the surface and shallow sub-surface of the plateau had been intensively
76 investigated (Gouyet, 1988; Campan, 1995; Greenroyd et al., 2007; Basile et al., 2013;
77 Pattier et al., 2013; 2015; Loncke et al., 2009, 2016; Mercier de Lépinay, 2016; Tallobre et
78 al., 2016; Fanget et al. 2020), the deeper part of the plateau, located under a thick
79 sedimentary cover was until recently (Nemčok et al., 2015; Reuber et al., 2016; Zinecker,
80 2020; Casson et al. 2021; Museur et al., 2021) studied less. The Guinea TMP has been less
81 well investigated but recent results are reported in: 1) Olyphant et al. (2017): the
82 southern Guinea Plateau and adjacent margin; Zinecker (2020): a new comparison of
83 Demerara and Guinea Plateaus structure and stratigraphy and Casson et al. (2021): high
84 resolution stratigraphic framework of post-rift evolution of the Demerara Plateau.

85 In this review paper, we use a combination of wide-angle seismic derived velocity
86 models, industrial seismic multi-channel data and line drawings of seismic lines, mainly
87 based on a recent thesis (Museur, 2020). We depict the state of the art of our knowledge
88 of the deep crustal structure and nature of the Demerara Plateau and their continuity with
89 the Guinea Plateau. These results allow to discuss the possible role of crustal inheritance,
90 thermal anomalies and superposed tectonic phases in formation of TMPs by the
91 comparison with other TMPs and volcanic margins, which share numerous characteristics
92 with the Demerara Plateau. Finally, we propose a simplified two-fold tectonic evolution
93 scheme for both TMPs over time.

94 **1. Geological context**

95 96 1.1. Origin of TMPs

97 The Demerara and Guinea conjugate TMPs (Figure 1) have been identified as
98 conjugate TMPs among about twenty marginal plateaus (Loncke et al., 2020) worldwide.

99 TMPs often share a complex tectonic history since they frequently combine different
100 rifting phases and distinct magmatic events. So far, many different geological processes
101 have been proposed to explain the evolution of TMPs. Some of them result from a hotspot-
102 influenced evolution comparable to Volcanic Passive Margins (VPM) such as the Walvis
103 Ridge in the South Atlantic (Chauvet et al., 2020). Similarly, the Falklands-Malvinas TMP
104 underwent a volcanic episode during its Lower Jurassic break-up in association with the
105 Karoo hotspot province (Barker, 1999; Schimschal & Jokat, 2018, 2019), while the second
106 phase of opening in the Lower Cretaceous led to the creation of the largest transform
107 margin in the world (Loncke et al., 2020). In the northern North Atlantic, the Hatton-
108 Rockall TMP underwent a phase of volcanic underplating (Klingelhoefer et al, 2005; White
109 et al., 2008, White & Smith, 2009,) and/or the development of a volcanic margin (Welford
110 et al., 2012) during its second opening phase. On the other hand, other TMPs remain
111 poorly known partly due to their inaccessibility (e.g. the Gunnerus Ridge: Leitchenkov et
112 al., 2008).

113

114 1.2. Kinematic reconstructions

115 The Demerara and Guinea conjugate TMPs result from a two-fold breakup history.
116 First, the western Demerara and Guinea margins formed during the Jurassic Central
117 Atlantic ocean opening; later, the Demerara and Guinea TMPs separated by transform
118 motion related to the highly oblique Cretaceous opening of the Equatorial Atlantic ocean
119 (Klitgord & Schouten, 1986; Benkhelil et al., 1995; Campan, 1995; Labails et al., 2010;
120 Moulin et al., 2010; Nemčok et al., 2015; Reuber et al., 2016).

121 Prior to the opening of the Central Atlantic Ocean, the Guyana shield, a vast
122 province extending from Venezuela to Amapá (mostly composed of rocks emplaced
123 during the Trans-Amazonian orogeny between 2.26 and 1.95 My in Paleoproterozoic
124 times), was the western extension of the Western Africa craton within Gondwana. It is
125 worth noting that the opening of the Central Atlantic Ocean was predated by a major
126 magmatic episode corresponding to the Central Atlantic Magmatic Province (CAMP;
127 Marzoli et al., 1999). It is a region of intense magmatic activity dated at 200 My, extending
128 over 2.5 million square kilometers and expressed in Guyana and Guinea by dense
129 networks of doleritic dykes

130 Later, the opening of the Central Atlantic separates North America and Africa
131 approximately following the Hercynian orogeny from the Newfoundland fracture zone in
132 the north (south of Grand Banks to the west, south of Iberia to the east) to Guyana-
133 Suriname in the south (Klitgord et Schouten, 1986), and was characterized by a NW-SE
134 (Figure 2) opening direction (Nemčok et al., 2015). At 170 My, after rifting, the Guinea and
135 Demerara Plateaus formed the eastern divergent margin of the southern Central Atlantic
136 ocean (Figure 2) facing the Bahamas platform and the Blake Plateau to the North (Pindell
137 and Kennan, 2009). It is precisely this phase that led to the formation of the western
138 continental margin of the Demerara Plateau along the eastern side of the Guyana Basin
139 (Labails et al., 2010; Nemčok et al., 2015) (Figure 2), which corresponds to a small piece
140 of the Jurassic Atlantic Ocean preserved from subduction below the Antilles.

141 According to Pindell & Kennan (2009), the Guyana Basin and the proto-Caribbean
142 seaway were shifted by a major transform zone (the Guyana Transform). At 124 My
143 (Figure 2), the North American, South American and Northwest African plates formed a
144 triple junction at the transition from the Central Atlantic to the Equatorial Atlantic
145 tectonic phases (Pindell & Kennan, 2009; Campan, 1995; Labails et al., 2010). Later (e.g.
146 104 My, Figure 2), the triple junction allowed the connection between the Central Atlantic,

147 a proto Caribbean domain already connected to the Central Atlantic at Jurassic times, and
148 the newly opened Equatorial Atlantic gateway (Pindell & Kennan, 2009). Splitting
149 between the Guinea and Demerara Plateaus results from the opening of this new
150 Cretaceous oceanic domain (Figure 2, 104 My) possibly following the trace of Panafrican
151 orogeny suture (Villeneuve & Cornée, 1994).

152 The Equatorial Atlantic rifting and early seafloor spreading occurred during the
153 Early Barremian to Aptian (Basile et al., 2005) and extending into Albian (Sapin et al.,
154 2016; Mercier de Lépinay et al., 2016; Olyphant et al., 2017) in a complex oblique mode,
155 connecting the laterally shifted Central Atlantic and South Atlantic oceanic domains
156 (Figure 1), with a change of the opening direction (Campan, 1995). Demerara and Guinea
157 plateaus initially slid apart in a dextral transform mode when the first oceanic crust is
158 proposed to have formed during the late Aptian (circa 115 My) (Basile et al., 2005). Later,
159 at 105 My, a slight modification in the oceanic opening direction may have resulted in the
160 oblique separation of Demerara and Guinea plateaus and would explain why from that
161 time oceanic transform zones are slightly oblique to the Demerara and Guinea transform
162 margins (Campan, 1995; Basile et al., 2013; Nemčok et al., 2015; Reuber et al., 2016)
163 (Figure 2). On the contrary, our latest vertical gravity maps (work in progress) tend to
164 show that the real transform segments of the Demerara Plateau are completely parallel to
165 fracture zones further east.

166

167 1.3. The Demerara Plateau

168 The Demerara TMP is a 230 km long, 170 km wide submarine high off French
169 Guiana and Suriname continental shelves (Figure 1). Previous investigations include
170 seismic surveys and multibeam bathymetry (Gouyet, 1988; Loncke et al., 2009; Basile et
171 al., 2013; Pattier et al., 2013, 2015; Loncke et al., 2016; Sapin et al., 2016; Fanget et al.,
172 2020) but also wide-angle seismics (Greenroyd et al., 2007, 2008; Museur et al., 2021)
173 and ODP drilling (Erbacher et al., 2004; Mosher et al., 2007).

174 Nowadays, the Demerara TMP exhibits three margins (Figure 1): (1) its western
175 border corresponds to a Jurassic divergent margin, (2) its northern border corresponds
176 to a Cretaceous transform margin, and (3) its eastern border to a Cretaceous divergent
177 margin (Gouyet, 1988; Basile et al., 2013; Nemčok et al., 2015; Sapin et al., 2016; Museur
178 et al., 2021).

179 Superficial structures include series of stacked Mass Transport Deposits (MTDs)
180 or deep-seated collapses along the plateau that have recorded a history of large-scale
181 slope failures (Loncke et al., 2009; Pattier et al., 2013, 2015) resulting from the
182 combination of the fluid overpressure, the internal geometry of the margin, the presence
183 of a steep transform margin, suitable décollement rheologies at various stratigraphic
184 levels (Pattier et al., 2015), and, at least, since Miocene, the action of deep bottom
185 thermohaline currents regularly eroding the slope (Fanget et al., 2020).

186 Within the plateau, Gouyet (1988), Benkhelil et al. (1995), Basile et al. (2013), and
187 Mercier de Lépinay, 2016 described the Cretaceous deformation mainly as characterized
188 by E-W to WNW-ESE trending folds related to wrench-related deformations due to a
189 period of transpression dated latest Aptian/early Albian, and sealed and peneplained by
190 a regional and prominent unconformity from the Upper Albian (Gouyet, 1988, Erbacher
191 et al., 2004 and Basile et al., 2013). The narrow continent to ocean transition of the eastern
192 margin (Sapin et al., 2016) is formed by a few tilted blocks with thick fan-shaped Aptian
193 to Mid-Albian syn-rift deposits. Subsequently, the breakup unconformity is proposed to
194 be Mid-Albian in age (~104 My) and correlates laterally with the major sub-aerial

195 environment related to the Upper Albian unconformity mentioned above. Post-Albian
196 sediments are 4 km thick below the continental shelf and progressively thin towards the
197 northern outer edge of the Demerara Plateau, forming a thick prograding wedge.

198 The northern slope of the plateau, corresponding to the transform margin,
199 provides a natural cross section through the deeper part of the plateau, outcropping at
200 the seafloor. Along this border, dredges of DRADEM cruise (Basile et al., 2017) have
201 recovered magmatic rocks: basalts, rhyolites (dated to 173.4 ± 1.6 My i.e. Basile et al.,
202 2020), trachy-basalts and basaltic trachy-andesites. All samples share similar trace
203 element composition (Basile et al., 2020). They are Light Rare-Earth Element-enriched,
204 and contain positive anomalies in Nb, Ta, Zr and Hf, typical of ocean island basalts (OIB),
205 and thus indicate a possibly hotspot-related magmatic event supporting the volcanic
206 origin of a part of the plateau (Reuber et al., 2016).

207 The deep structure of the Demerara Plateau was first imaged by wide-angle
208 seismic data, along a 500 km SSW-NNE oriented line (Greenroyd et al., 2007, 2008) which
209 enabled the Demerara Plateau to be interpreted as a sliver of continental crust thinned
210 during the opening of the Central Atlantic and later reworked orthogonally by the
211 transform Equatorial Atlantic opening. The Demerara Plateau was also imaged by
212 industrial deep-penetrating reflection seismic lines, which unequivocally revealed the
213 existence of very thick and wide Seaward Dipping Reflector (SDR) packages thickening
214 towards the Jurassic Central Atlantic domain (Reuber et al., 2016). To the west below the
215 SDRs Reuber et al. (2016) proposed the existence of an enigmatic “volcanic igneous crust”
216 formed by magmatic processes during the Jurassic opening in relation to the SDR wedges
217 formation. Alternatively, in particular to the east, this might also represent a geological
218 unit pre-dating the opening of the Central Atlantic and including a basement composed in
219 part of meta-sediments corresponding to the Guiana Shield (Precambrian craton)
220 (Mercier de Lépinay et al., 2016). A second set of data from better resolved wide-angle
221 and reflection seismic experiments confirmed this observation and documented a 30 km
222 thick crust under the Demerara Plateau with velocities fitting those of a LIP (Large
223 Igneous Province)-type crust (Museum et al., 2021). Nemčok et al. (2015), Reuber et al
224 (2016) and Museum et al. (2021) proposed that the the Demerara Plateau is part of an
225 inherited Jurassic volcanic margin bordering the southern end of the Central Atlantic
226 Ocean, which may have resulted from the Sierra Leone hotspot activity localized in the
227 Demerara area at the end of the Lower Jurassic (Basile et al., 2020).

228
229

1.4. The Guinea Plateau

230 The less investigated Guinea TMP (Figure 1) is a 220 km long, 120 km semi-circular
231 submarine high off Guinea-Bissau and Guinea. Nowadays the Guinea TMP exhibits two
232 margins (Figure 1): (1) its western border corresponding to a divergent Jurassic margin
233 related to the Central Atlantic ocean opening, (2) its southern border corresponding to a
234 Cretaceous transform margin related to the Equatorial Atlantic ocean opening (Figure 2).
235 Because of this location, the Mesozoic structure and stratigraphy of the Guinea Plateau
236 recorded the combined effects of an older Triassic-Jurassic rift event related to the
237 opening of the Central Atlantic ocean and a younger period of Aptian right-lateral shearing
238 along the Guinea fracture zone during the oblique opening of the Equatorial Atlantic ocean
239 (Klitgord & Schouten, 1986; Benkhelil et al., 1995; Basile et al., 2013; Olyphant et al., 2017)
240 (Figure 2).

241 Comprehensive geophysical studies of the entire Guinea Plateau are very recent
242 (Olyphant et al., 2017; Zinecker, 2020). Older works resulted in the seismic refraction data

243 over the south and western Guinea Plateau (Sheridan et al., 1969) and magnetic and
244 shallow reflection seismic data (McMaster et al., 1970). Mascle et al. (1986) presented an
245 updated bathymetric map of the Guinea margin showing the contrasting morphologies of
246 slopes. Based on the analysis of seismic data acquired in the eighties, Marinho et al. (1988)
247 and Benkhelil et al. (1995) expanded the Mascle et al. (1986) study and defined two
248 tectonic events affecting the southern Guinea Plateau: 1) rift-related normal faults
249 affecting the Albian and older sequences, and 2) folding, reverse faulting, and transcurrent
250 faulting of Late Cretaceous and older sequences that recorded structural inversion. This
251 inversion was followed by Cenozoic magmatism responsible for the emplacement of
252 numerous volcanoes located immediately south of the plateau and along the transform
253 border. Subsequently, Benkhelil et al. (1995) proposed a schematic reconstruction of the
254 relative location and tectonic evolution of the Demerara and Guinea TMPs by comparing
255 their observations with those of Gouyet (1988).

256 The Guinea Plateau has been sporadically the object of hydrocarbon exploration
257 since the 1960's, and hydrocarbon discoveries in the early 2000's along the passive
258 margins adjacent to the Guinea Plateau and the Demerara Rise have led to renewed
259 exploration activity (Sayers & Cooke, 2018). Based on recent 2D and 3D seismic datasets
260 and drills acquired on the southern Guinea Plateau and the Sierra Leone margin, Olyphant
261 et al., 2017 show that volcanics and basalts are widespread along the transform to
262 divergent corner off Guinea and Liberia. Their age is mainly Albian but early Aptian
263 basalts have also been drilled. These emplace mainly in relation with Aptian to Albian
264 rifted tilted blocks. Olyphant et al. (2017) emphasize the asymmetry of rifting between
265 Demerara and Guinea areas.

266 **2. Published data**

267 Data synthesized in this paper stem from two datasets. Firstly, academic deep
268 penetrating multichannel reflection and wide-angle seismic data from the Demerara
269 Plateau acquired during the MARGATS (IUEM/Ifremer) oceanographic experiment on the
270 R/V L'Atalante in 2016 were modeled and interpreted (Museum et al., 2021). Secondly, a
271 dataset of industrial Multi-Channel Seismic (MCS) lines including several sets of deep-
272 penetrating reflection seismic data, some of them imaging down to 16 s (TWT), covering
273 the Demerara and Guinea Plateaus.

274 During the MARGATS experiment, 80 ocean-bottom seismometers (OBS) were used
275 for 171 deployments. They were deployed along four combined reflection and wide-angle
276 seismic profiles, two of which are discussed in this study (Figure 1). We used a 6500 cubic
277 inch airgun array seismic source fired every 60 seconds corresponding to a 150 m shot
278 spacing. In this paper we present two-way time converted velocity models from the
279 eastern part of the Plateau (Figure 2) derived from wide-angle seismic and coincident
280 academic MCS for comparison with industrial MCS data (Figures 3 and 4): the NE-SW
281 MAR01 (56 OBS) profile crossing the eastern divergent margin at its intersection with the
282 northern transform margin and the WNW-ENE MAR02 (37 OBS) profile intersecting the
283 eastern divergent margin. Coincident MCS Margats data are used to control geometries of
284 upper layers. They were pre-processed on board using the *SolidQC* software from Ifremer
285 and processing was completed in the laboratory using either *Geovation* software (CGG) or
286 *SeisSpace ProMax*. The processing included filtering, deconvolution, NMO correction,
287 stacking, velocity analysis, and time migration. Detailed analysis and presentation of the
288 wide-angle data can be found in Museum et al. (2021). Wide-angle data were modeled
289 using the RAYINVR forward modeling software (Zelt & Smith, 1992). The superficial

290 layers (from the seafloor down to the top of the crust) were further constrained by
291 bathymetric data and the coincident MCS data. We used a minimum structure/parameter
292 approach to avoid inclusion of structures unconstrained by the data and gravity modeling
293 to test the broad structure of the velocity models. Details of modelling processes, error
294 estimation and coincident gravity modeling used to verify and extend the seismic models
295 are presented in Museur et al. (2021).

296 Combined line drawings from the Demerara Plateau presented in this paper result
297 from interpretation of industrial MCS data including (Figure 1): 1) ION Geophysical
298 GuyanaSPAN 2D seismic survey. The survey images the plateau and its margins in water
299 depths of 40-3500 m and was provided by TOTAL SA in two-way travel time (TWT) cut at
300 16 seconds. Pre-stack depth converted sections were published in Reuber et al. (2016)
301 and Casson et al., 2021). 2) CGG MCS correspond to high quality 8 seconds data in TWT
302 covering the western Demerara Plateau. 3) Fugro seismic data set is composed of 5 km
303 spaced 12 s (TWT) lines covering the eastern part of the plateau and margin.

304 The age and nature of the different units is partially constrained by well data (Mercier
305 et al., 2016) and includes the Sinnamary, FG-2 and Demerara A2 wells (Figure 1).
306 Sinnamary (SE Demerara) penetrates post-Albian to Lower Cretaceous sedimentary
307 series, which are mainly composed of sands and claystones down to an undated basement
308 gneiss proposed to correspond to French Guianese Precambrian. The FG-2 well (eastern
309 Demerara) drilled through Post-Albian series, the Albian unconformity, Aptian to
310 Neocomian sediments down to Barremian basalts intercalated with sands (Gouyet, 1988).
311 The Demerara A2 well (western plateau) penetrates post-Albian claystones and
312 carbonates, the Albian unconformity down to shallow water claystones and carbonates
313 proposed to be either Aptian and Neocomian for the claystones and a Jurassic age
314 (Oxfordian) for the carbonates (Gouyet, 1988; Loncke et al., 2020), or Callovian for the
315 carbonates from alternative biostratigraphic interpretations (Nemčok et al., 2015;
316 Griffith, 2017). However, a more recent study (Casson et al., 2021) proposes an age no
317 older than late Tithonian based on calpionellid occurrence. In this study, we consider that
318 they correspond to a carbonate platform developed along the Central Atlantic Demerara
319 margin from late Jurassic to Neocomian.

320 The shelf, slope and deepwater areas of the Guinea Plateau, varying between 10 m to
321 4800 m water depth, have been mainly covered by TGS seismic surveys (2012, 2017),
322 although these data are not as good quality as the GXT lines. TGS lines were available
323 (courtesy TOTAL SA) down to 9 or 14 seconds TWT. The Continent Ocean Boundary is
324 poorly imaged. Some of these lines are shown in pre-stack depth migrated format in
325 Zinecker (2020) and Casson et al. (2021).

326 Overall, the combination of velocity and geometry of the layers allows a robust
327 interpretation and is used to propose the chronology and processes that led to the
328 formation of Demerara and Guinea plateaus.

329 **3. Results and synthesis**

330 **3.1. The Demerara Plateau**

331 *Velocity models*

332 We focus on the velocity distribution of model MAR01 (Figure 5a) because MAR01
333 and MAR02 (see Figure 1 for location) models show relatively similar structural patterns.
334 Detailed results and data can be found in Museur et al. (2021). Nevertheless, both models
335 are presented as two-way time-converted along composite lines D2 and D3 (Figures 3 and
336 4). The MAR01 model is composed of seven layers including: the water column, two

337 sedimentary layers, three underlying crustal layers, and the mantle layer. According to
338 lateral variations in layer thicknesses and velocity-depth laws (Figure 5), model was
339 divided into three parts: plateau, transition and ocean domains (Figure 5). Based on
340 velocities and gradients within the plateau domain, the 25 km thick deep crust can be
341 divided into three layers: upper crust, middle crust and lower crust. Velocities from top
342 of the upper crust and base of the middle crust range from 4.5 km/s to 7.0 km/s with a
343 significant gradient within the upper crust (Figure 5b). Velocity gradient within the upper
344 crust (0 to 6 km below sediments) is strong ~ 0.33 km/s/km, compared to its low value
345 within the middle crust (6 to 23 km) ~ 0.03 km/s/km, and intermediate value within the
346 lower crust (23 to 28 km) ~ 0.08 km/s/km. According to composite lines D2 (Figure 3)
347 and D3 (Figure 4), the upper part of the crust likely corresponds to a 20 km thick layer
348 comprised of a large complex of superimposed wedges (these wedges are part of the
349 Jurassic margin formed by magma-assisted extension) thickening toward the Jurassic
350 oceanic crust and proposed to be Seaward Dipping Reflectors SDRs (Reuber et al., 2016).
351 The lower unit is characterized by velocities significantly higher than mean continental
352 crust defined by Christensen & Mooney (1995), ranging from 7.2 to 7.6 km/s, its average
353 thickness is 5 km (in MAR01) and 7 km (in MAR02). Along MAR01, the lower crustal unit
354 rapidly tapers out from 230 km model distance toward the northeast (Figure 5a). Once
355 converted into two-way travel time, the Lower Unit in MAR02 forms an enigmatic shape
356 below the transition domain (Figure 3) toward the Equatorial Atlantic domain. The
357 oceanic domain is clearly identified and characterized by an approximately 5 km thick
358 crust along both profiles. It directly overlies the mantle. However, a comparison with
359 velocities and velocity gradients corresponding to normal oceanic crust (Figure 5d)
360 (White et al., 1992) indicates a magmatic origin of this crust.

361

362 *E-W and N-S trending composite lines*

363 To enhance the interpretation of composite lines D2 (Figure 3) and D3 (Figure 4)
364 which are partly coincident with the two velocity models MAR01 and MAR02, we used
365 additional MCS line drawings oriented approximately East - West (Figure 6) and North -
366 South (Figure 7). They cover the entire Demerara Plateau and reach the Equatorial and
367 Central Atlantic oceanic domains (see Figure 1 for location). The composite lines D2 and
368 D3 are divided into: the plateau domain, the western margin with the Central Atlantic
369 oceanic domain, and the north eastern transform and eastern rifted margins with the
370 adjacent Equatorial Atlantic oceanic domain.

371

372 • The plateau domain

373 The plateau domain (Figures 3 and 4) is well constrained in composite lines. The
374 upper part of the plateau is marked by a major erosional unconformity (Basile et al., 2013;
375 Fanget et al., 2020) below the post Albian strata. This overlying unit is affected by major
376 instabilities along the slopes of the plateau, especially in the north (Figure 7). These
377 features are beyond the scope of this paper and detail descriptions are given in Loncke et
378 al. (2009); Gaullier et al. (2010) and Pattier et al. (2015) and are synthesized in Fanget et
379 al. (2020).

380 Below the Albian unconformity, an Aptian-Albian unit irregularly covers the
381 Plateau and can be divided into two subsets. The first one is older in age and located on
382 the western part of the plateau (Figure 6). It is mainly located below the slope (D1 and
383 D2) in the north. It spans the western part of the plateau (D3) in the south. This subunit
384 can be more than two seconds thick. It is affected by numerous normal faults toward the

385 margin, which are related to major slope instabilities above a probably inherited Jurassic
386 relief. The second subunit appears stratigraphically younger in age and forms an
387 extensive basin generally thinning toward the east (Figure 6, D1, D2 and D3) and the
388 north-east where it is truncated. This subunit is affected by major compressive,
389 apparently meridian, deformation, forming long-wavelength folds and, in some cases,
390 related compressive faults (Figure 7, D4, D5 and D7). A detailed analysis of deformation
391 reveals WNW – ESE fold axes, generally parallel to the northern margin of the plateau. To
392 the north west, this subunit is affected by numerous extensive faults that cut through the
393 Albian unconformity and portion of the overlying post-Albian strata (Figure 7), possibly
394 due to a subordinate post-Albian extensional phase. The Albian erosional unconformity
395 represents a significant stratigraphic gap and seals the compressive deformation.

396 The Aptian/Albian units were deposited above a strong amplitude seismic facies
397 unit proposed to be Jurassic to Neocomian in age according to well FG2-1 (see Figure 1
398 for location), affecting the age span of the second subunit in Mercier de Lépinay (2016).
399 This unit reaches a maximum of ~ 3 s (TWT) thickness in the northwestern part of the
400 Plateau (Figure 6, D2 and Figure 7, D4) and progressively thins toward the east where it
401 pinches out in the eastern part of the plateau (Figure 6) and toward the south (Figure 7).
402 The Jurassic-Neocomian unit is affected by the compressional deformation described
403 above. The base of the sequence is often represented by an erosional unconformity
404 described as the post-rift Jurassic unconformity (Figures 6 and 7)

405 The lower part of the plateau below the post-rift unconformity is composed of fan
406 shaped units outlined by relatively continuous and high amplitude reflectors described as
407 Seaward (westward) Dipping Reflectors (SDRs). The whole set of SDRs lies on the deeper
408 identified crustal Unit A. According to the velocity models, these SDR units reach a
409 maximum thickness of ~ 7 s (TWT) or about 22 km (Figures 3 and 4) and spread over ~
410 450 km from west to east (Figure 6). They can be divided into the Lower SDR, and the
411 Upper SDR 1 and 2 that represent different shapes and regional extents. The Lower SDR
412 unit lies on the Unit A to the east, while in the west, Unit A is covered with either Upper
413 SDR 1 or 2. Thus, the base of SDRs is diachronous and contains faults that control the
414 emplacement and growth of SDR bodies (Figure 6). Looking perpendicularly at the D4 and
415 D5 sections (Figure 7) SDR units appear as basin shaped structures with no coincident
416 depocenters. Lines D6 (Figure 6) and D7 (Figure 7) from the eastern part of the plateau
417 reveal significant thickness of Lower SDR unit and a possible magmatic source causing
418 symmetric SDR bodies to be emplaced. According to the velocity models (Figures 3 and
419 4), the western part of SDRs corresponds to the upper and middle crust of the velocity
420 models providing a velocity range from 4.5 to 7 km/s between the Upper and Lower SDRs.
421 Unexpectedly, the velocity structure is very stable and flat across the eastern part of the
422 plateau (Figures 3 and 4) compared to the geometry evidenced by MCS data. It raises the
423 question of the significance of velocity variations with concern to their related rock
424 natures at those sites. In fact, the boundary between SDRs and Unit A is not detectable in
425 the velocity models. In contrary to MCS lines, a distinction between SDR units and the
426 underlying unit A is based on a change in seismic facies: from continuous and strong
427 reflectors of SDR units to rather chaotic facies occasionally marked by strong amplitudes
428 that may correspond to magmatic intrusions characterizing Unit A.

429 Below Unit A, we propose two laterally adjacent lower units (Figures 3 and 4). To
430 the east, along velocity models MAR01 and MAR02, the existence of a deep high velocity
431 layer (Lower Unit 2) with values ranging from 7.2 to 7.6 km/s (Figure 5) is required to fit
432 the arrivals observed in OBS records (Museum et al., 2021). To the west, the Lower Unit 1

433 corresponds to poorly reflective facies on MCS data. At this stage, there is neither proven
434 nor obvious connection between these lower units.

435

436 • Western rifted margin and adjacent Central Atlantic oceanic domain starting with
437 Jurassic crust

438 Along the western rifted margin (see Figure 1 for location), the Albian erosional
439 unconformity and overlying layers mark the upper limit to the deformation. Below the
440 outer western slope, the lowest levels of Post-Albian units are only deformed by few
441 extensional faults (Figure 6).

442 The underlying Aptian-Albian unit reaches a thickness of ~ 3.5 s (TWT) above the
443 present-day slope (Figure 6, D1) where it is also characterized by major west-dipping
444 extensional faults that belong to major gravity driven slides in Cretaceous strata. On
445 section D2 (Figure 6), the result of slope instabilities, probably controlled by an inherited
446 topography of the Jurassic-Neocomian carbonate platform, is characterized by a bulge
447 shape and a thick set of discontinuous deposits that progressively thin toward the basin.

448 The thickness of the Jurassic-Neocomian unit appears to be controlled by erosive
449 processes involving slope failure above the present-day margin (Figure 6, D2) with a clear
450 thinning along a paleo-slope toward the oceanic domain where it seems to fill up a graben-
451 like structure at the transition between the interpreted oceanic crust (Figure 6, D2 and
452 D3) and the western enigmatic margin crust (western extension of Unit A). The western
453 edge of the carbonate platform over the volcanic series (SDRs) was already a major slope
454 break that probably controlled the future slope evolution and hence its apparent spatial
455 stability in time. On sections D2 and D3 (Figure 6) and with no equivalent to the north
456 (D1), the Jurassic-Neocomian unit covers the underlying outer SDR unit toward the
457 oceanic domain with a rather constant ~ 1 s (TWT) thickness.

458 The following lower part of the western margin is marked by the beveling of Upper
459 SDR 1 and 2 toward the west above the possible extent of Unit A (Figure 6). However, an
460 adjacent fan-shaped body, which also shares acoustic and geometric characteristics with
461 SDRs, is located between the western end of the Upper SDR Unit and the interpreted
462 oceanic domain (Figure 6, D2 and D3). This unit is called "Outer SDR" because of its
463 location outside the plateau domain and above the more distal extent of Unit A.

464 Below unit A, the Lower Unit 1 is only well-imaged below the western margin on
465 line D3 (Figure 6) where it thins toward the west. The onset of Jurassic oceanic crust is
466 proposed on the western flank of the graben-like structure where the Moho flattens to the
467 west. This transition is much more enigmatic on line D1 (Figure 6).

468

469 • Eastern rifted and northern transform margins of the plateau and adjacent Atlantic
470 Equatorial oceanic domain starting with Cretaceous oceanic crust

471 The eastern margin is only partially, but well imaged by the eastern part of D2
472 section (Figure 6). The velocities are constrained by the sub-coincident MAR02 velocity
473 model (Figure 3). It looks like a relatively narrow (less than 130 km) divergent margin
474 composed of a few crustal tilted blocks covered with fan-shaped syn-Cretaceous rift
475 sediments, and controlled by east-dipping normal faults. However, due to the difficulty to
476 follow the Albian unconformity over the transitional domain, it is difficult to define which
477 part of the Albian Cretaceous strata represents a syn-rift phase. The Jurassic-Neocomian
478 unit

479 appears to pinch out and onlap to the east rather than being truncated, suggesting that it
480 was never present to the east. However, the western limit of the eastern transitional zone
481 seems to coincide with the more easterly extent of Jurassic SDR bodies (Figure 6) over

482 Unit A. A coincident wide-angle velocity model reveals that within SDRs and Unit A,
483 velocities are depth-dependent and not controlled by stratigraphy (Figure 3). To the east
484 of the SDRs limit, Unit A forms the substratum of post Neocomian units, including post-
485 Albian units, in a tectonically-controlled depositional system. According to MAR02
486 velocity model, Unit A is above the high velocity (7.2 to 7.4 km/s) Lower Unit 2, which
487 reaches a thickness of 2–4 s (TWT) and ends toward the adjacent Cretaceous oceanic
488 crust, well constrained by MAR02 velocity model.

489 The northeastern margin of the plateau corresponds to the outer corner at the
490 junction between the transform segment and the divergent segment described above (see
491 Figure 1 for location). It is well imaged by the northeastern part of the composite line D3
492 (Figure 6), and constrained by velocities of the sub-coincident MAR01 velocity model
493 (Figures 4 and 5). It forms a wider transitional domain composed of a crustal block
494 deformed by a system of faults with both dips directions, controlling depocenters, and
495 filled with syn-tectonic (rift – transform) post-Neocomian – pre-Albian sediments (Figure
496 6, D3). The relation between extent of the transitional zone, SDRs and Unit A is very
497 similar to that of line D2. Once again, velocities appear to be depth-dependent and not
498 related to geometry of individual rock units, as documented by coincident MCS (Figure 4,
499 D3). In depth, the Lower Unit 2 in profile D3 is thinner than in profile D2, i.e. around 1–2
500 s (TWT). To the north-east, the distal part of the transitional domain (Figure 4), prior to
501 the unambiguous and thin oceanic crust (5 km, Figure 5), represents a domain of
502 uncertain type. It shares some velocity characteristics with oceanic domain but its
503 structural layout is more compatible with Unit A. Thus, this transitional domain makes it
504 difficult for one to draw a precise Continent Ocean Boundary (COB) in this outer corner
505 area.

506 The northern border of the plateau is considered to correspond to the Equatorial
507 Atlantic transform margin (see Figure 1 for location). It is well depicted by the
508 northeastern part of lines D4 and D5 in Figure 7. This margin corresponds to a very abrupt
509 and steep transition between the plateau domain and the adjacent Equatorial Atlantic
510 oceanic domain, which starts with Cretaceous crust. The Albian unconformity seals the
511 deformation occurring in the region from the plateau down to the adjacent basin as a post-
512 transform discontinuity. Below the plateau edge, the unconformity truncates the entire
513 folded Aptian – Albian sequence and a part of the Jurassic-Neocomian sequence (Figure
514 7). Along the slope, the transform fault zone cuts through the deeper units including SDRs
515 and Unit A. In depth, Unit A forms a prominent basement ridge. In section D5 (Figure 7),
516 moderately deformed Lower SDR and Upper SDR 1 onlap the southern flank of the ridge.
517 In section D4 (Figure 6) to the west, Lower SDR and Upper SDR 1 appear to be more
518 deformed and tilted to the south thanks to a possible basement ridge uplift. However,
519 Lower SDR and Upper SDR 1 still onlap the ridge. In accordance to this observation, we
520 consider that the basement ridge must have existed, at least partly, prior to the first SDRs
521 emplacement.

522
523

3.2. The Guinea Plateau

524 The network of seismic profiles covering the Guinea Plateau is far less dense than
525 that on the Demerara Plateau. For comparison, a quick overview based on three seismic
526 sections G1, G2 and G3 (Figure 8) is given in order to explore the possible continuity of
527 deep geological structures from the Demerara TMP to the Guinea TMP.

528 The opening of Equatorial Atlantic has been widely debated (Moulin et al, 2010 and
529 references therein). The authors propose a new model from the tightest reconstruction to

530 Chron C34. For the more precise understanding of the relative positions of the Demerara
531 Plateau, Mercier de Lepinay (2016) proposed reconstructions obtained using the rotation
532 poles of Moulin et al. (2010) and constrained by COB alignment and correlation between
533 carbonate platforms and Albian slope instabilities. Despite the uncertainties in COB
534 location and inspired by the above studies, we propose a visual hand-made morphological
535 reconstruction that aims to connect similar geological units on either side of the
536 Equatorial Atlantic opening trajectory (Figure 9).

537 Section G1 (see Figure 1 for location) is oriented WNW-ESE, presumably along the
538 extension of section D4 from the Demerara Plateau (Figures 8 and 9). It images the crust
539 down to 9 s (TWT). Our seismic interpretation reveals 5 major units. The upper (light-
540 yellow) unit (Figure 8) forms a young sedimentary prism corresponding to post-Albian
541 strata. It is separated from the older Cretaceous sequence by a major unconformity
542 (green) that is the upper limit to a moderate deformation of the underlying layers as
543 shown by the truncating reflectors. It looks very similar to the Albian unconformity
544 described at the Demerara Plateau (Figure 9). The unit below the unconformity shows a
545 less reflective facies that is slightly folded. It is characterized by a relatively homogeneous
546 thickness of ~ 1.5 s (TWT). It is proposed to correspond to the Alptian/Albian unit of the
547 Demerara Plateau (Figure 9). It covers a homogeneous unit (blue in Figure 8) displaying
548 long parallel reflectors with strong amplitude, which thickens from 1 to 1.5 s (TWT)
549 toward the SSW. It shows similar characteristics to the Jurassic-Neocomian unit of the
550 Demerara Plateau. The underlying unit (pink in Figure 8) is composed of strong amplitude
551 reflectors, slightly tilted to the SSW. It shares numerous characteristics with the Demerara
552 SDR wedges (Figure 9). Its deeper unit shows a very low amplitude, contrasting with the
553 overlying SDR sequence. It may match with a lateral equivalent of Unit A described at the
554 Demerara Plateau (Figure 9). The last unit (orange in Figure 8) shows pale seismic facies
555 which vertically penetrates through all the other units from a depth of ~ 7 s (TWT) to the
556 top of post-Albian units. It corresponds to a salt diapir, rooting below the SDR units. This
557 stratigraphic salt level occurs in several basins of the Guinea Plateau and has been dated
558 to ~ 190 My (Jansa et al., 1980; Wade & MacLean, 1990). A juxtaposition of lines D4 and
559 G1 (Figure 9) reveals a relative continuity and symmetry of the upper units. It also
560 indicates the asymmetry of SDR bodies due to contradictory evolution of the underlying
561 Unit A, forming a prominent substratum ridge along the northern border of the Demerara
562 Plateau.

563 Section G2 (see Figure 1 for location) is oriented SW – NE, presumably in the
564 basement extension of line D5 from the Demerara Plateau according to our simple
565 reconstruction (Figure 9). It images the Guinea Plateau down to 14 s (TWT) and more or
566 less shows the same vertical unit stacking, with a notable difference concerning the
567 possible Jurassic-Neocomian unit and the less clear Albian unconformity. This section
568 underlines the overall thickening of Guinea SDR bodies toward the SW, where they reach
569 a total thickness of 4.5 s (TWT). The Moho is possibly located between depths of 11.5 and
570 13 s (TWT). The juxtaposition of lines D5 and G2 (Figure 9) confirms a remarkable
571 continuity of Cretaceous and Jurassic sedimentary units and also the major asymmetry
572 related to the basement ridge in Unit A in depth. Finally, the Moho depth is coherent
573 between the Demerara and Guinea TMPs. The attenuated late Cretaceous deformation
574 observed in G1 is imperceptible in the southeastern part of the Guinea Plateau and still
575 much more severe in the northwestern Demerara Plateau (Figure 9).

576 Section G3 (see Figure 1 for location) is oriented WNW – ESE (Figure 8). It has been
577 chosen to be compared to the structure of a similarly oriented line through the Demerara
578 Plateau (Figure 9, D1). Section G3 shows a 9 s (TWT) section of the Guinea Plateau

579 structure. The same 5 main units with specific geometry are present. It is worth noting
580 that the SDR bodies show a similar westward thickening. The base of the SDR unit is
581 difficult to determine on the Guinea Plateau. However, the SDRs reach a thickness of least
582 ~ 4 s (TWT), slightly less than the similar unit of the Demerara Plateau. Subsequently, it
583 is hard to determine a possible lateral continuity of specific SDR units, such as the Lower
584 SDR, that clearly pinch out against the basement ridge made in Unit A (Figure 9). The line
585 also images the western border of the Guinea Plateau, which is marked by a distinct relief
586 inherited from the Jurassic history of the margin that seems to control the emplacement
587 of the interpreted Aptian/Albian units. The Albian unconformity limits the residual relief
588 that is covered by the post-Albian strata. According to depth-converted interpretation of
589 similarly oriented seismic line through the Guinea Plateau, Zinecker (2020) proposed that
590 the basement unit underlying Mesozoic and Cenozoic sequences is of oceanic crustal
591 nature. Therefore, we suggest a similar interpretation along line G3 (Figure 8).
592 Additionally, a comparison with line D1 from the Demerara Plateau shows a similar
593 organization of the different units (Figure 9).

594 **4. Discussion**

595 The aforementioned results help to specify and discuss: 1) the deep structure and
596 nature of the Demerara TMP and their implications for the knowledge of emplacement
597 and evolution of similar TMPs, 2) the origin and evolution of both the Guinea and
598 Demerara TMPs.

599 4.1. Deep structure of conjugated TMPs

600 *Deep structure of the Demerara Plateau*

601

602 The proposed velocity models (Figures 3, 4 and 5) complement the first wide-angle
603 study of the plateau from Greenroyd et al. (2007), which was designed to image the
604 central western plateau. Our and their results are generally consistent in terms of
605 velocities and unit thicknesses. However, our results provide a new insight in deep
606 structural architecture, thanks to a large number of OBSs employed and the volume of the
607 seismic source. In fact, the top of our new deep unit, represented by the high velocity
608 Lower Unit, corresponds to the Moho interpreted by Greenroyd et al. (2007). At the same
609 time, Reuber et al. (2016) pointed out the unambiguous existence of thick SDRs in the
610 western part of the Plateau as previously suggested by Nemčok et al. (2015) and Mercier
611 de Lépinay et al. (2016). Composite lines (Figures 3 and 4) help to correlate velocity
612 models with reflection seismic results in order to provide additional constraints on the
613 deeper layers including SDRs.

614 The deep structure of the Demerara Plateau is composed of three layers: SDRs, Unit
615 A and Lower Unit. The upper part of the crust corresponds to a wide, generally westward-
616 dipping (thickening) wedge of SDRs. They are proposed to be composed of varying
617 mixtures of subaerial volcanic flows, and volcano-clastic and non-volcanic sediments (see
618 Okay, 1995; Menzies, 2002) that can be divided into different structural types mainly
619 based on geometric criteria (see Chauvet et al., 2020). Our SDR set is divided into Lower
620 SDR, and Upper SDR 1 and 2, with significantly different velocity characteristics: Upper
621 SDR between 4.5 and 6 km/s with a major vertical gradient and Lower SDR between 6
622 and 7 km/s (Figure 5). However, our velocity models do not show major lateral variations.
623 At the same depth, the Lower SDR has similar velocities as the Upper SDR (5 km/s at ~ 8 -

624 9 km depth; 6.5 km/s at about 18 km depth). This fact negates the hypothesis that the
625 proportion of sediment in the SDRs could explain such velocity variations (Paton et al.,
626 2017). Subsequently, the velocity may be mainly controlled by depth and pressure (White
627 et al., 1992) even if some other processes may be involved, such as: weathering or
628 hydrothermal alteration, increasing the proportion of intrusive rocks. The emplacement
629 of the SDRs appears to be controlled by major landward-dipping extensional faults
630 (Figure 6) according to Gibson & Love (1989); Eldholm et al. (1995); Geoffroy et al. (2015)
631 and Chauvet et al. (2020) more than being flexure-related due to dykes or sills loading
632 (Mutter et al., 1982; Planke & Eldholm, 1994; Paton et al., 2017).

633 According to composite lines D2 and D3 and the velocity models (Figures 3 and 4),
634 the physical limit between SDRs and Unit A represents a very low acoustic impedance
635 contrast. Unit A is proposed to be a pre-Jurassic continental crust possibly representing
636 the Guyana Shield, injected by magmatic intrusions possibly related to volcanic events
637 responsible for the formation of the SDRs or older events related to CAMP (Bullard et al.,
638 1965; May, 1971; Deckart et al., 1997; Marzoli et al.; 1999; McHone, 2000; Deckart et al.,
639 2005). Alternative interpretation can include a neoformed crust as suggested before
640 (Gernigon et al., 2004; Reston, 2009) in a similar context, such as in the Vøring Basin
641 where magma-affected middle crust or even magmatic crust like that of the Namibian
642 Margin (Bauer et al., 2000) exhibit higher velocities at similar depths (7–7.5 km/s).

643 Lower Units 1 and 2 (Figures 3 and 4) have been determined from MCS data and
644 wide-angle data respectively. Even if the thicknesses and depths are compatible, the lack
645 of data in the central plateau casts doubt on their link and continuity. Wide-angle data
646 help to constrain a velocity range from 7.2 to 7.6 km/s, comparable to a High Velocity
647 Lower Crust (HVLC) proposed by Geoffroy et al. (2015). Such velocity ranges have been
648 variously interpreted as 1) serpentinized mantle (O'Reilly et al., 2006), 2) volcanic
649 underplated unit (Planert et al., 2017), and 3) pre-rifting continental crust intruded by a
650 large amount of magmatic products (Abdelmalak et al., 2016). Clear reflected P waves
651 from the Moho (PmP) at the base of Lower Unit observed on OBS data (Museum et al.,
652 2021) reject the serpentinized mantle hypothesis. According to the shape, velocities and
653 geometry, Lower Unit 1 clearly corresponds to a HVLC typical for volcanic margins
654 (Geoffroy et al., 2015) and would, therefore, be related to Jurassic rifting. It can be either
655 a pre-rifting continental crust intruded by a major amount of magmatic products, or an
656 underplated magmatic material. In contrast, Lower Unit 2 has a more proximal position
657 in respect to the Jurassic margin, and exhibits a greater thickness (3–4 s (TWT), 6–7 km
658 according to Figure 5). It is located below the Cretaceous eastern divergent margin.
659 Consequently, Lower Units 1 and 2 may have different origins. The Lower Unit 2 may have
660 resulted from a distinct Cretaceous magmatic event compatible with volcanic sills
661 proposed by Sapin et al. (2016) in the eastern transition domain and Barremian basaltic
662 rocks found in well FG2–1 (Mercier de Lépinay et al., 2016).

663 664 *Comparison with various crustal structures and geometries*

665
666 The Demerara Plateau velocity structure is compared to velocity depth structures
667 (Figure 5) of selected TMPs from Loncke et al. (2020) and LIP-type Plateau near the
668 Agulhas TMP (Parsiegla et al., 2007). On one hand, the Demerara TMP, the Agulhas TMP,
669 the Walvis TMP, the Faroe Bank and the Hatton-Rockall TMP (Parsiegla et al., 2007; Funck
670 et al., 2008; White & Smith, 2009; Fromm et al., 2017) show similar trends with depth and
671 contain comparable thicknesses that clearly differ their crust from the continental crust
672 (Christensen & Mooney, 1995). On the other hand, the velocity depth structures of the

673 Falklands-Malvinas TMP (Schimschal & Jokat, 2018; 2019) and the Agulhas Plateau
674 (Parsiegla et al., 2007) are very different from those of the above-mentioned group,
675 having clearly higher velocities and smaller thicknesses. Within the heterogeneous
676 structure of the Falklands-Malvinas TMP (Schimschal & Jokat, 2018; Schimschal & Jokat,
677 2019), only the Maurice Ewing Bank's internal block has a comparable velocity depth
678 structure.

679 Comparison of the Demerara Plateau velocity structure (Figure 5) with the SE
680 Greenland (Hopper et al., 2003) and the Namibian volcanic margins (Bauer et al., 2000)
681 reveal strong similarities with TMPs of the first group. Moreover, the Namibian margin
682 velocities in the upper crust and the lower crust are equivalent to those observed at the
683 Demerara Plateau, whereas the middle crust slightly differs, possibly as a consequence of
684 the composition and intrusive magmatism (Schön, 1996; Bauer et al., 2000).

685 Following, we compare (Figure 10) the key elements of the deep structure of the
686 Demerara Plateau (Figure 10 a) including: SDRs, Unit A, Lower Unit (HVLC), with those of
687 the Hatton-Rockall TMP (Figure 10 b), the Walvis TMP (Figure 10 c) and the Faroe Bank
688 (Figure 10 d), all of which show a similar three-layer organization (Figure 10 b, c and d),
689 forming comparable 25–33 km-thick plateaus even though different in width. In
690 particular, the Walvis Ridge, characterized by the presence of an SDR complex (Elliott et
691 al., 2009; Jegen et al., 2016; McDermott et al., 2018, Chauvet et al., 2020) a possibly thick
692 (about 33 km), dominantly gabbroic crust (Planert et al. 2017), is interpreted as a volcanic
693 margin associated with a hotspot trail (Gladchenko et al. 1998; Elliott et al. 2009). The
694 Walvis Ridge shows characteristics very similar to the Demerara Plateau. They both share
695 similar structural characteristics with well documented volcanic margins such as the
696 Pelotas (Figure 10 f) and Namibian (Figure 10 g) margins (Bauer et al., 2000; Fernandez
697 et al., 2010; Stica et al., 2014; Jegen et al., 2016; Planert et al., 2017) containing: 1) an SDR-
698 dominated upper crust, 2) a middle crust called igneous crust or transitional crust
699 possibly representing a pre-SDR crust strongly intruded by magma (Bauer et al., 2000;
700 Fromm et al., 2017; Planert et al., 2017), and 3) a HVLC.

701 From another point of view, the second group composed by Falklands-Malvinas
702 and Agulhas Plateaus (Figures 5 and 10 e) clearly differs from the Demerara Plateau.
703 Going from west to east, the heterogeneous Falklands-Malvinas Plateau consists of the
704 Falklands- Malvinas Plateau basin represented by a 12–20 km overthickened oceanic
705 domain, a possible “continental” domain represented by the Maurice-Ewing Bank and the
706 Georgia Basin oceanic domain (Schimschal & Jokat, 2019) where only the Maurice-Ewing
707 Bank shows similar velocities to those of the Demerara Plateau (Figure 5). On the other
708 hand, the Agulhas Plateau, which is defined as a LIP type “oceanic” plateau (Parsiegla et
709 al., 2007), looks very similar to the Falklands-Malvinas TMP, with no evidence of either
710 SDR complexes or HVLC even if their formation is also related to the influence of a hotspot
711 i.e. the Karoo Hotspot (Linol et al., 2015; Hole et al., 2015).

712 To conclude, the first group of TMPs and volcanic margins shares the characteristic
713 of being under hotspot influence, which explains SDR bodies and HVLC emplacement
714 (Fowler et al., 1989; Geoffroy, 2005; White et al., 2008; Elliott et al., 2009), like the Iceland
715 hotspot for Faroe Bank and Rockall-Hatton TMPs (Elliott et al., 2009). However, some
716 other plateaus located in the South Atlantic Ocean, such as Falklands-Malvinas and
717 Agulhas TMPs, seem to result from a different evolution, indicating that not all TMPs
718 identified by Loncke et al. (2020) were formed by the same process.

719 Finally, our analysis leads to proposing that the structure of the Demerara Plateau
720 corresponds to a Jurassic volcanic margin (see also Nemčok et al., 2015), which raises the
721 question of the origin of the major volcanic products, and suggesting the possible

722 presence of a hotspot for the Demerara Plateau, and subsequently, the Guinea region in
723 early Jurassic. This hypothesis is confirmed by seismic data (Reuber et al., 2016) and
724 geochemical analyses and dating of deep seafloor samples by Basile et al. (2020).

725 4.2. Evolution of the Demerara – Guinea conjugated TMPs

726 Based on our results, we present a schematic evolution of both conjugate plateaus
727 in cross sections (Figure 11). According to kinematic plate reconstructions (Figure 2),
728 before the opening of Central Atlantic, the Demerara-Guinea was facing to the north west
729 the present-day Bahamas platform, Florida and, possibly, the Blake Plateau (Figure 2).
730 Few deep penetrating seismic data are available in this area of the North America margin,
731 but a recent compilation of gravimetric and seismic data (Dale, 2013) indicated a wide 20
732 km-thick domain of anomalous high-density crust located between the continental crust
733 of Florida and the Central Atlantic oceanic crust. Density values are between 2.8 and 2.9
734 g/cm³, comparable to those obtained for SDR units after conversion from wide-angle
735 velocities (Museum et al., 2021). Therefore, the authors interpret this domain as an
736 enigmatic LIP transitional crust. Our data also help to prove the continuity of magmatic
737 units from Demerara to Guinea plateaus (Figures 9 and 11).

738 Reuber et al. (2016) were the first to propose a hotspot to explain the SDRs and the
739 subsequent amount of volcanic products for Demerara, and proposed that this hotspot
740 was located close to the Bahamas, to the west of the Demerara Plateau during the Jurassic
741 period. They named it the “Bahamas hotspot”. A long-lived hotspot activity generally
742 results in a major volcanic expression forming a hotspot track according to plate motion
743 (Morgan & Chen, 1993), which has not yet been documented for the Demerara Plateau
744 case. During the DRADDEM experiment (Basile et al., 2017), dredge samples were obtained
745 along the steep northern transform margin of the plateau, which allowed the deeper levels
746 to be reached. The samples reveal the geochemical signature typical for ocean island
747 basalts (OIB). Their zircon dates to 173.4 ± 1.6 My (Basile et al., 2017). Based on these
748 data, Basile et al., (2020) proposed a hotspot-related magmatic event, associated with the
749 opening of the Central Atlantic and not related to the anterior CAMP volcanism (about 200
750 My old) at the beginning of the Demerara Plateau development.

751 Subsequently, Basile et al. (2020) drew a possible hotspot track, which was initially
752 located below the Demerara Plateau at 170 My. It was possibly later responsible for the
753 formation of the Sierra Leone Rise (Figures 2 and 5). According to this model, the
754 Demerara Plateau may be located back above this same hotspot in the Cretaceous period.
755 If the hypothesis concerning the possibly conjugate Bahamas-Florida margin is right,
756 together with the Demerara – Guinea plateaus this area was corresponding to a large
757 magmatic province 400 km long in the north-south direction and 600 km wide in the east-
758 west direction, resulting from the Jurassic “Sierra Leone” hotspot activity.

759 This hotspot would have been responsible for the formation of the Demerara and
760 Guinea volcanic margins. The presence of 190 My-old salt diapirs rooting below SDR units
761 in the Guinea Plateau confirms (see datings in Basile et al., 2020) that the SDR body
762 emplacement in the Guinea and Demerara region postdates the CAMP event (Figure 11)
763 and supports the hotspot hypothesis (Reuber et al., 2016; Basile et al., 2020) with a peak
764 event at 170 My (Basile et al., 2020). The maximum thickness of the SDR units is reached
765 in the south-western Demerara Plateau and in the continuity with the present-day
766 southern margin of the Guinea Plateau (Figure 11), even though they are separated by the
767 basement ridge. We propose (Figure 11) that this prominent ridge represents a
768 preexisting crustal relief located at the junction between the two plateaus without

769 preventing emplacement of SDR units. Our results also illustrate the possibility of an
770 aborted magmatic rift axis in the actual central eastern plateau (Figures 6 and 11),
771 demonstrating the complex occurrence and polyphase tectonically-controlled
772 emplacement of SDR bodies.

773 Later, during the early Cretaceous, the second phase of the history of the Guinea and
774 Demerara Plateaus started with the development of the Equatorial Atlantic rift, possibly
775 along pre-existing lithosphere zone of weakness and basement ridge (Figures 2 and 11).
776 After the Jurassic evolution marked by a major post-SDR Jurassic unconformity and
777 before the second rifting phase (Mercier de Lépinay et al., 2016), the sediment supply
778 compensated the post-rift subsidence with the emplacement of the Jurassic-Neocomian
779 carbonate platform along the possibly inherited relief of the volcanic margin. During
780 Barremian/Aptian, an acceleration of subsidence is reported. A large delta characterized
781 by gravity-driven tectonics formed west of both plateaus (Figure 11). Then, the rifting
782 phase culminated by the progressive breakup between the Demerara and Guinea
783 plateaus. It was delivered by a dextral shearing along a major transform fault system
784 accompanied by deformation (Figure 2 and 11). Alongside, the eastern Demerara
785 divergent margin is facing the Sierra Leone divergent margin. In fact, this narrow (<90
786 km) eastern margin of the Demerara Plateau (Figure 6) is deformed by eastward dipping
787 normal faults bounding tilted blocks with depocenters filled by Cretaceous pre-late Albian
788 sediments. The proximal part of this margin remarkably coincides with the easternmost
789 extension of the SDR complex, which may have resulted from a localization of the
790 deformation between blocks of various rheologies (Figure 11). In the transitional domain,
791 (Figure 6) no evidence of an exhumed mantle has been found (Sapin et al., 2016).
792 However, there is a possible underplated high velocity unit (Lower Unit 2), which may
793 have resulted from the second rifting phase related to the Cretaceous volcanic event due
794 to the influence of the same hotspot that was associated with the Jurassic opening (as
795 proposed by Basile et al. (2020)).

796 During the Albian, both plateaus experienced major uplift and deformation. The
797 main deformation characterized by E-W to WNW-ESE trending folds (Figure 6) was
798 demonstrated by Gouyet (1988), Benkhelil et al. (1995), Basile et al. (2013), Mercier de
799 Lépinay (2016). This deformation in the Guinea Plateau is far less recorded than it is in
800 the Demerara Plateau, even though some evidence can be seen on line G1 (Figure 8). The
801 major deformation seems to have then concentrated in the northern part of the Demerara
802 Plateau, south of the basement ridge (Figure 7), which acted as a buttress to the
803 transpressive tectonics preceding the final separation of the Demerara and Guinea
804 Plateaus. In fact, folds are sometimes cut by transform related normal faults (Loncke et
805 al., 2021). Subsequently, the transpressive tectonics is proposed to be Aptian/early Albian
806 in age. It is related to the evolution of the stress field as a consequence of a possible
807 rotation pole shift at Aptian-Albian limit (Rabinowitz & Labrecque, 1979; Campan, 1995;
808 Basile et al., 2013; Reuber et al., 2016.). This led to the collision of the north of the
809 Demerara area with the southwest of the Guinea area (Figure 11). Finally, the ultimate
810 continental separation have led to a general collapse of the margin (Figure 11), cut by the
811 regional and prominent upper Albian unconformity in its upper part.

812 **5. Conclusions**

813 This work brings new insights on the nature and the emplacement of the transform
814 conjugate Demerara and Guinea Plateaus, thanks to wide angle seismic data and a
815 compilation of industrial reflection seismic data. Analysis of these data reveals that

816 Demerara and Guinea Plateaus once were a Jurassic volcanic margin. It formed the
817 segment of the eastern Central Atlantic margin. It was composed of thick SDR units,
818 intruded continental crust, and a high velocity lower crust. However, emplacement of the
819 SDRs was diachronous with a possible aborted first volcanic source and tectonically
820 controlled by a pre-existing basement ridge. This magmatic system is proposed to be
821 controlled by the activity of the “Sierra Leone” hotspot.

822 This large magmatic province was reworked during the Cretaceous opening of the
823 Equatorial Atlantic. A major transform transform fault zone developed the Northern
824 margin of the Demerara Plateau and the Southern margin of the Guinea Plateau. The
825 opening of the Equatorial Atlantic was predated by a compressive event recorded in the
826 Demerara Plateau. The location of the transform margin appears to be controlled by the
827 pre-existing basement grain whereas the Eastern rifted margin of the Demerara Plateau
828 seems to have been located along the eastern limit of the Jurassic SDR units.

829 This work also discusses the characteristics of the Demerara-Guinea volcanic
830 margin and subsequent TMPs by a comparison to similar TMPs in the Atlantic Ocean, such
831 as the Walvis Ridge. However, not all TMPs share the same characteristics, as is
832 exemplified by the Falklands-Malvinas and Agulhas TMPs. On the other hand, the western
833 Jurassic margin of the Demerara TMP looks very similar to the Namibian and Pelotas
834 volcanic margins. Of course, not all TMPs and volcanic margins have been imaged by
835 equally robust seismic data sets. Subsequently, future studies of the structure and nature
836 of different TMPs and volcanic margins are required to precisely explore and quantify
837 common processes leading to their formation such as hotspots-related major thermal
838 anomalies and superposed tectonic phases.

839

840 **Acknowledgments**

841 We thank the captain and crew of the R/Vs “*L’Atalante*” for the data acquisition during
842 marine survey MARGATS. Further information and some data are available on the
843 internet site of the French Oceanographic Fleet.

844 (<https://campagnes.flotteoceanographique.fr/campagnes/16001400/fr/>). T. Muséum
845 PhD Thesis was funded by the Regional Council of Bretagne and Ifremer. Access to
846 industry MCS data was provided by TOTAL SA. Thanks to Gplates (Muller et al., 2018),
847 Qgis, Generic Mapping Tools (Wessel and Smith, 1991), Gravity from Sandwell and Smith
848 (2009) for figures realization.

849 We thank reviewers for their very helpful reviews.

850

851 **References**

852

853 Abdelmalak, M. M., Planke, S., Faleide, J. I., Jerram, D. A., Zastrozhnov, D., Eide, S., & Myklebust, R., 2016. The
854 development of volcanic sequences at rifted margins: New insights from the structure and
855 morphology of the Vøring Escarpment, mid-Norwegian Margin. *Journal of Geophysical Research:*
856 *Solid Earth*, 121(7), 5212-5236.

857 Barker, P. F., 1999. Evidence for a volcanic rifted margin and oceanic crustal structure for the Falkland
858 Plateau Basin. *Journal of the Geological Society*, 156 (5): 889-900.
859 <https://doi.org/10.1144/gsjgs.156.5.0889>

860 Basile, C., Mascle, J., & Guiraud, R., 2005. Phanerozoic geological evolution of the Equatorial Atlantic domain.
861 *Journal of African Earth Sciences*, 43(1-3), 275-282.

862 Basile, C., Maillard, A., Patriat, M., Gaullier, V., Loncke, L., Roest, W., Mercier de Lépinay, M., Pattier, F., 2013.
863 Structure and evolution of the Demerara Plateau, offshore French Guiana: rifting, tectonic inversion
864 and post-rift tilting at transform- divergent margins intersection. *Tectonophysics* 591, 16-29.

- 865 Basile, C., Girault, I., Heuret, A., Loncke, L., Poetisi, E., Graindorge, D., Deverchère, J., Klingelhoefer, F., Lebrun,
866 J.F., Perrot, J., & Roest, W., 2017. Morphology and lithology of the continental slope north of the
867 Demerara marginal Plateau: results from the DRADEM cruise. EGUGA, 8107
- 868 Basile, C., Girault, I., Paquette, J.L., Agranier, A., Loncke, L., Heuret, A., Poetisi, E., 2020. The Jurassic
869 magmatism of the Demerara Plateau (offshore French Guiana) as a remnant of the Sierra Leone
870 hotspot during the Atlantic rifting. *Sci. Rep.* 10 (1), 1–12.
- 871 Bauer, K., Neben, S., Schreckenberger, B., Emmermann, R., Hinz, K., Fechner, N., Gohl, K., Schulze, A.,
872 Trumbull, R., Weber, K., 2000. Deep structure of the Namibia continental margin as derived from
873 integrated geophysical studies. *J. Geophys. Res.* 105, 25829–25854. [https://doi.org/10.1029/
874 2000JB900227](https://doi.org/10.1029/2000JB900227).
- 875 Benkhelil, J., Mascle, J., Tricart, P., 1995. The Guinea continental margin: an example of a structurally
876 complex transform margin. *Tectonophysics* 248, 117–137. [https://doi.org/10.1016/0040-
877 1951\(94\)00246-6](https://doi.org/10.1016/0040-1951(94)00246-6)
- 878 Bullard, E., Everett, J.E., Smith, A.G., 1965. The fit of the continents around the Atlantic. In: Bickett, P.M.S.,
879 Bullard, E., Runcorn, S.K. (Eds.), *A Symposium on Continental Drift*, Philos. Trans. R. Soc. Lond., A, vol.
880 258, pp. 41–51.
- 881 Campan, A., 1995. *Analyse Cinématique de l'Atlantique Equatorial, Implications Sur l'évolution de
882 L'atlantique Sud et sur la Frontière de Plaque Amérique du Nord/ Amérique du Sud*. PhD Thesis. Univ.
883 "Pierre et Marie Curie", Paris VI (352 pp).
- 884 Casson, M., Jeremiah, J., Calvès, G., de Goyet, F. D. V., Reuber, K., Bidgood, M., ... & Redfern, J., 2021. Evaluating
885 the segmented post-rift stratigraphic architecture of the Guyanas continental margin. *Petroleum
886 Geoscience*, 27(3).
- 887 Chauvet, F., Sapin, F., Geoffroy, L., Ringenbach, J. C., & Ferry, J. N., 2020. Conjugate volcanic passive margins
888 in the austral segment of the South Atlantic—Architecture and development. *Earth-Science Reviews*,
889 103461.
- 890 Christensen, N.I., Mooney, W.D., 1995. Seismic velocity structure and composition of the continental crust:
891 a global view. *J. Geophys. Res.* 100 (B6), 9761–9788. <https://doi.org/10.1029/95JB00259>.
- 892 Dale, A. J. (2013). *Crustal type, tectonic origin, and petroleum potential of the Bahamas carbonate platform
893 (Doctoral dissertation)*
- 894 Deckart, K., Bertrand, H., Liégeois, J.-P., 2005. Geochemistry and Sr, Nd, Pb isotopic composition of the
895 Central Atlantic Magmatic Province (CAMP) in Guyana and Guinea. *Lithos* 82, 282–314.
896 <https://doi.org/10.1016/j.lithos.2004.09.023>.
- 897 Deckart, K., Féraud, G., Bertrand, H., 1997. Age of Jurassic continental tholeiites of French Guyana, Surinam
898 and Guinea: implications for the initial opening of the Central Atlantic Ocean. *Earth Planet. Sci. Lett.*
899 150, 205–220.
- 900 Eldholm, O., Skogseid, J., Planke, S., Gladchenko, T.P., 1995. Volcanic margin concepts. Springer 463.
901 https://doi.org/10.1007/978-94-011-0043-4_1.
- 902 Elliott, G., Berndt, C., Parson, L., 2009. The SW African volcanic rifted margin and the initiation of the Walvis
903 Ridge, South Atlantic. *Marine Geophysical Research*. 30. 207-214. 10.1007/s11001-009-9077-x.
- 904 Erbacher, J., Mosher, D.C., Malone, M.J., Sexton, P., Wilson, P.A., 2004. *Proceedings of the Ocean Drilling
905 Program, Initial Reports. Vol. 207. Demerara Rise: equatorial Cretaceous and Paleogene
906 paleoceanographic transect, Western Australia. Covering Leg 207 of the cruises of the Drilling Vessel"
907 Joides Resolution", Bridgetown, Barbados, to Rio de Janeiro, Brazil, Sites 1257-1261, 11 January-6
908 March 2003. Texas A & M University Ocean Drilling Program.*
- 909 Fanget, A.N., Loncke, L., Pattier, F., Marsset, T., Roest, W., Tallobre, C., Durrieu de Madron, X., Hernández-
910 Molina, F., 2020. A synthesis of the sedimentary evolution of the Demerara Plateau (Central Atlantic
911 Ocean) from the late Albian to the Holocene. *Marine and Petroleum Geology*. 104195.
912 10.1016/j.marpetgeo.2019.104195.
- 913 Fernandez, M., Afonso, J., Ranalli, G., 2010. The deep lithospheric structure of the Namibian volcanic
914 margin. *Tectonophysics* 481. <https://doi.org/10.1016/j.tecto.2009.02.036>.
- 915 Fowler, S.R., White, R.S., Spence, G.D., Westbrook, G.K., 1989. The Hatton Bank continental margin—II. Deep
916 structure from two-ship expanding spread seismic profiles. *Geophysical Journal International* 96 (2),
917 295–309.
- 918 Fromm, T., Jokat, W., Ryberg, T., Behrmann, J., Haberland, C., Weber, M., 2017. The onset of Walvis Ridge:
919 Plume influence at the continental margin. *Tectonophysics* 716, 90–107.
920 <https://doi.org/10.1016/j.tecto.2017.03.011>.
- 921 Funck, T., Morten Sparre, A., Neish, J., Dahl-Jensen, T., 2008. A refraction seismic transect from the Faroe
922 Islands to the Hatton-Rockall Basin. *J. Geophys. Res.* 113 <https://doi.org/10.1029/2008JB005675>.

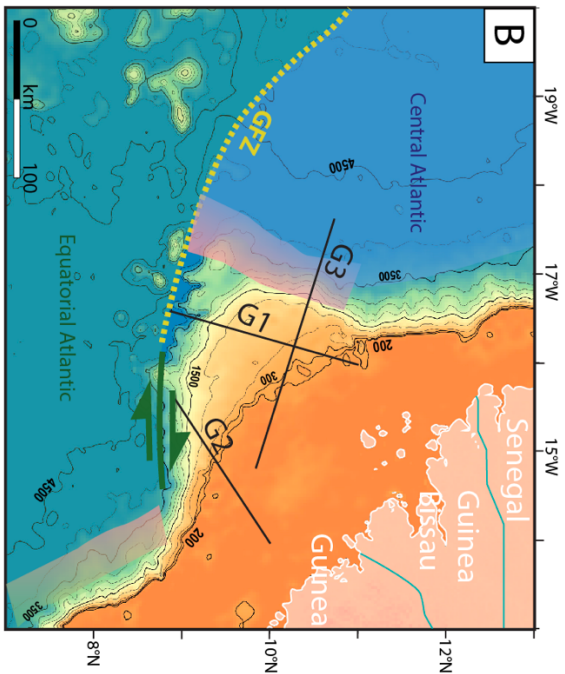
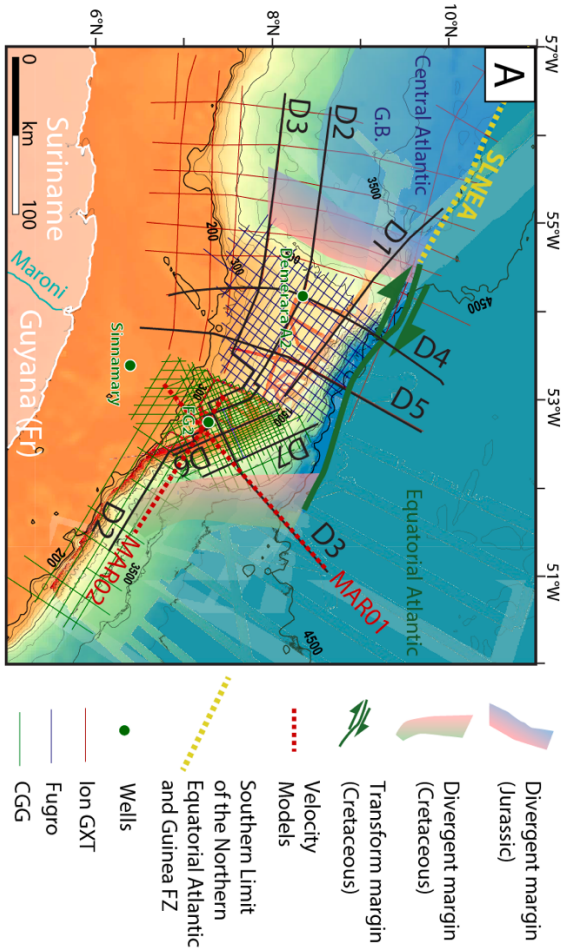
- 923 Gaullier, V., Loncke, L., Droz, L., Basile, C., Maillard, A., Patriat, M., ... & Carol, F., 2010. Slope instability on the
924 French Guiana transform margin from swath-bathymetry and 3.5 kHz echograms. In *Submarine Mass*
925 *Movements and Their Consequences* (pp. 569-579). Springer, Dordrecht.
- 926 Geoffroy, L., 2005. Volcanic passive margins. *Comptes Rendus Geoscience*, 337(16), 1395-1408.
- 927 Geoffroy, L., Burov, E.B., Werner, P., 2015. Volcanic passive margins: another way to break up continents.
928 *Sci. Rep.* 5 (1), 1-12.
- 929 Gernigon, L., Ringenbach, J.C., Planke, S., Le Gall, B., 2004. Deep structures and breakup along volcanic rifted
930 margins: insights from integrated studies along the outer Vøring Basin (Norway). *Marine and*
931 *Petroleum Geology* 21(3), 363-372.
- 932 Gibson, I., Love, D., 1989. A listric Fault Model for the Formaztion of the Dipping Reflectors Penetrated
933 during the Drilling of the Hole 642E, ODP 104. *Scientific Results* 104, 979-983.
934 <https://doi.org/10.2973/odp.proc.sr.104.195.1989>.
- 935 Gladczenko, T. P., Skogseid, J., & Eldhom, O., 1998. Namibia volcanic margin. *Marine geophysical researches*,
936 20(4), 313-341.
- 937 Gouyet, S., 1988. Évolution tectono-sédimentaire des marges guyanaise et nord-brésilienne au cours de
938 l'évolution de l'Atlantique Sud. PhD Thesis. Univ. " Pau et des pays de l'Adour " (374 pp).
- 939 Graindorge, D., Klingelhofer, F., 2016. MARGATS cruise, RV
940 L'Atalante, <https://doi.org/10.17600/16001400>
- 941 Greenroyd, C. J., Peirce, C., Rodger, M., Watts, A. B., & Hobbs, R. W., 2007. Crustal structure of the French
942 Guiana margin, west equatorial Atlantic. *Geophysical Journal International*, 169(3), 964-987.
- 943 Greenroyd, C. J., Peirce, C., Rodger, M., Watts, A.B., Hobbs, R.W., 2008. Demerara Plateau- the structure and
944 evolution of a transform passive margin. *Geophysical Journal International* 172, 549-564.
945 <https://doi.org/10.1111/j.1365-246X.2007.03662.x>
- 946 Griffith, C.P., 2017. Evidence for a Jurassic Source Rock in the Guiana-Suriname Basin. AAPG
947 Datapages/Search and Discovery Article #90291, AAPG Annual Convention and Exhibition, Houston,
948 Texas, April 2-5, 2017.
- 949 Hole, M., Ellam, R., Macdonald, D., Kelley, S., 2015. Gondwana break-up related magmatism in the Falkland
950 Islands. *J. Geol. Soc.* <https://doi.org/10.1144/jgs2015-027>.
- 951 Hopper, J.R., Dahl-Jensen, T., Holbrook, W.S., Larsen, H.C., Lizarralde, D., Korenaga, J., Kelemen, P.B., 2003.
952 Structure of the SE Greenland margin from seismic reflection and refraction data: Implications for
953 nascent spreading center subsidence and asymmetric crustal accretion during North Atlantic
954 opening. *Journal of Geophysical Research: Solid Earth* 108 (B5).
- 955 Jansa, L. F., Bujak, J. P., & Williams, G. L., 1980. Upper Triassic salt deposits of the western North Atlantic.
956 *Canadian Journal of Earth Sciences*, 17(5), 547-559.
- 957 Jegen, M., Avdeeva, A., Berndt, C., Franz, G., Heincke, B., Hoř z, S., Kopp, H., 2016. 3-D magnetotelluric image
958 of offshore magmatism at the Walvis Ridge and rift basin. *Tectonophysics* 683, 98-108.
- 959 Klingelhofer, F., Edwards, R. A., Hobbs, R. W., and England, R. W., 2005. Crustal structure of the NE Rockall
960 Trough from wide-angle seismic data modeling, *J. Geophys. Res.*, 110, B11105,
961 doi:10.1029/2005JB003763.
- 962 Klitgord, K. D., and Schouten, H., 1986. Plate kinematics of the central Atlantic. *in* (Vogt, P. R., and Tucholke,
963 B. E. Eds.), *The Geology of North America, Volume M, The Western North Atlantic Region*, Geological
964 Society of America, 351-378.
- 965 Labails, C., Olivet, J.-L., Aslanian, D., Roest, W.R., 2010. An alternative early opening scenario for the Central
966 Atlantic Ocean. *Earth and Planetary Science Letters* 297, 355-368.
967 <https://doi.org/10.1016/j.epsl.2010.06.024>
- 968 Leitchenkov, G., Guseva, J., Gandyukhin, V., Grikurov, G., Kristoffersen, Y., Sand, M., Aleshkova, N., 2008.
969 Crustal structure and tectonic provinces of the Riiser-Larsen Sea area (East Antarctica): results of
970 geophysical studies. *Marine Geophysical Research*, 29(2), 135- 158.
- 971 Linol, B., deWit, M.J., Guillocheau, F., Robin, C., Dauteuil, O., deWit, M.J., Guillocheau, F., deWit, M.J.C., 2015.
972 Multiphase Phanerozoic subsidence and uplift history recorded in the Congo Basin: a complex
973 successor basin. In: *Geology and Resource Potential of the Congo Basin*. Springer-Verlag, Berlin
974 Heidelberg, pp. 213-227.
- 975 Loncke, L., Droz, L., Gaullier, V., Basile, C., Patriat, M., & Roest, W., 2009. Slope instabilities from echo-
976 character mapping along the French Guiana transform margin and Demerara abyssal plain. *Marine*
977 *and Petroleum Geology*, 26(5), 711-723.
- 978 Loncke, L., Droz, L., Gaullier, V., Basile, C., Patriat, M., & Roest, W., 2009. Slope instabilities from echo-
979 character mapping along the French Guiana transform margin and Demerara abyssal plain. *Marine*
980 *and Petroleum Geology*, 26(5), 711-723.

- 981 Loncke, L., Maillard, A., Basile, C., Roest, W. R., Bayon, G., Gaullier, V., Marsset, T., 2016. Structure of the
982 Demerara passive-transform margin and associated sedimentary processes. Initial results from the
983 IGUANES cruise. Geological Society, London, Special Publications, 431(1), 179-197.
- 984 Loncke, L., Roest, W.R., Klingelhoefer, F., Basile, C., Graindorge, D., Heuret, A., Marcaillou, B., Museur, T.,
985 Fanget, A.S., Mercier de Lépinay, M., 2020. Transform Marginal Plateaus. *Earth-Science Reviews* 203,
986 102940. <https://doi.org/10.1016/j.earscirev.2019.102940>
- 987 Loncke, L., de Lépinay, M. M., Basile, C., Maillard, A., Roest, W. R., De Clarens, P., ... & Sapin, F. (2021).
988 Compared structure and evolution of the conjugate Demerara and Guinea transform marginal
989 plateaus. *Tectonophysics*, 229112.
- 990 Marinho, M., Mascle, J., & Wannesson, J. (1988). Structural framework of the southern Guinean margin
991 (central Atlantic). *Journal of African Earth Sciences (and the Middle East)*, 7(2), 401-408.
- 992 Marzoli, A., Renne, P. R., Piccirillo, E. M., Ernesto, M., Bellieni, G., and De Min, A., 1999. Extensive 200-million-
993 year-old continental flood basalts of the Central Atlantic Magmatic Province, *Science*, 284(5414),
994 616- 618.
- 995 Marzoli, A., Renne, P. R., Piccirillo, E. M., Ernesto, M., Bellieni, G., and De Min, A., 1999. Extensive 200-million-
996 year-old continental flood basalts of the Central Atlantic Magmatic Province, *Science*, 284(5414), 616-
997 618.
- 998 Mascle, J., Marinho, M. and Wannesson, J., 1986. The structure of the Guinean continental margin:
999 implications for the connection between the central and the South Atlantic oceans. *Geol. Rundschau*,
1000 75(1), 57-70.
- 1001 May, P.R., 1971. Patterns of Triassic diabase dikes around the North Atlantic in the context of predrift
1002 position of the continents. *Geol. Soc. Am. Bull.* 82, 1285–1292.
- 1003 McDermott, C., Lonergan, L., Collier, J. S., McDermott, K. G., & Bellingham, P., 2018. Characterization of
1004 Seaward-Dipping Reflectors Along the South American Atlantic Margin and Implications for
1005 Continental Breakup. *Tectonics*, 37(9), 3303-3327.
- 1006 McHone, G.J., 2000. Non-plume magmatism and rifting during the opening of the Central Atlantic Ocean.
1007 *Tectonophysics* 316, 287–296.
- 1008 McMaster, R. L., Lachance T. P., and Ashraf, A., 1970. Continental shelf geomorphic features off Portuguese
1009 Guinea, Guinea, and Sierra Leone (West Africa), *Marine Geology*, 9, 203-213.
- 1010 Menzies, M.A. (Ed.), 2002. Volcanic rifted margins, vol. 362. Geological Society of America.
- 1011 Mercier de Lépinay, M., 2016. Inventaire mondial des marges transformantes et évolution tectono-
1012 sédimentaire des plateaux de Demerara et de Guinée. PhD Thesis. Univ. Perpignan.
- 1013 Mercier de Lépinay, M., Loncke, L., Basile, C., Roest, W. R., Patriat, M., Maillard, A., & De Clarens, P., 2016.
1014 Transform continental margins—Part 2: A worldwide review. *Tectonophysics*, 693, 96–115.
1015 <https://doi.org/10.1016/j.tecto.2016.05.038>
- 1016 Morgan, J. P., and Chen, Y. J., 1993. The genesis of oceanic crust: Magma injection, hydrothermal circulation,
1017 and crustal flow, *J. Geophys. Res.*, 98(B4), 6283– 6297, doi:10.1029/92JB02650.
- 1018 Mosher, D.C., Erbacher, J., Malone, M.J. (Eds.), 2007. Proceedings of the Ocean Drilling Program, 207
1019 Scientific Results, Proceedings of the Ocean Drilling Program. Ocean Drilling Program.
1020 <https://doi.org/10.2973/odp.proc.sr.207.2007>
- 1021 Moulin, M., Aslanian, D., Unternehr, P., 2010. A new starting point for the South and Equatorial Atlantic
1022 Ocean. *Earth-Science Reviews* 98, 1–37. <https://doi.org/10.1016/j.earscirev.2009.08.001>
- 1023 Müller, R. D., Cannon, J., Qin, X., Watson, R. J., Gurnis, M., Williams, S., et al. 2018. GPlates: Building a virtual
1024 Earth through deep time. *Geochemistry, Geophysics, Geosystems*, 19. doi:10.1029/2018GC007584.
- 1025 Museur, T., Graindorge, D., Klingelhoefer, F., Roest, W. R., Basile, C., Loncke, L., & Sapin, F., 2021. Deep
1026 structure of the Demerara Plateau: From a volcanic margin to a Transform Marginal
1027 Plateau. *Tectonophysics*, 803, 228645.
- 1028 Museur, T., 2020. Caractérisation de la structure profonde du Plateau de Démérara, au large de la Guyane et
1029 du Suriname. PhD Thesis. Univ. Bretagne Occidentale (247 pp).
- 1030 Mutter, J.C., Talwani, M., Stoffa, P.L., 1982. Origin of seaward-dipping reflectors in oceanic crust off the
1031 Norwegian margin by “subaerial sea-floor spreading”. *Geology* 10(7), 353–357.
- 1032 Nemčok, M., Rybár, S., Odegard, M., Dickson, W., Pelech, O., Ledvényiová, L., Matejová, M., Molčan, M.,
1033 Hermeston, S., Jones, D., Cuervo, E., Cheng, R. and Forero, G., 2015. Development history of the
1034 southern terminus of the Central Atlantic; Guyana-Suriname case study. In: Nemčok, M., Rybár, S.,
1035 Sinha, S. T., Hermeston, S. A. and Ledvényiová, L., (Eds), 2015. Transform margins: development,
1036 controls and petroleum systems. Geological Society of London Special Publication No 431,
1037 <http://doi.org/10.1144/SP431.10>.
- 1038 Okay, Nilgun, 1995. Thermal Development and Rejuvenation of the Marginal Plateaus along the
1039 Transtensional Volcanic Margins of the Norwegian-Greenland Sea.

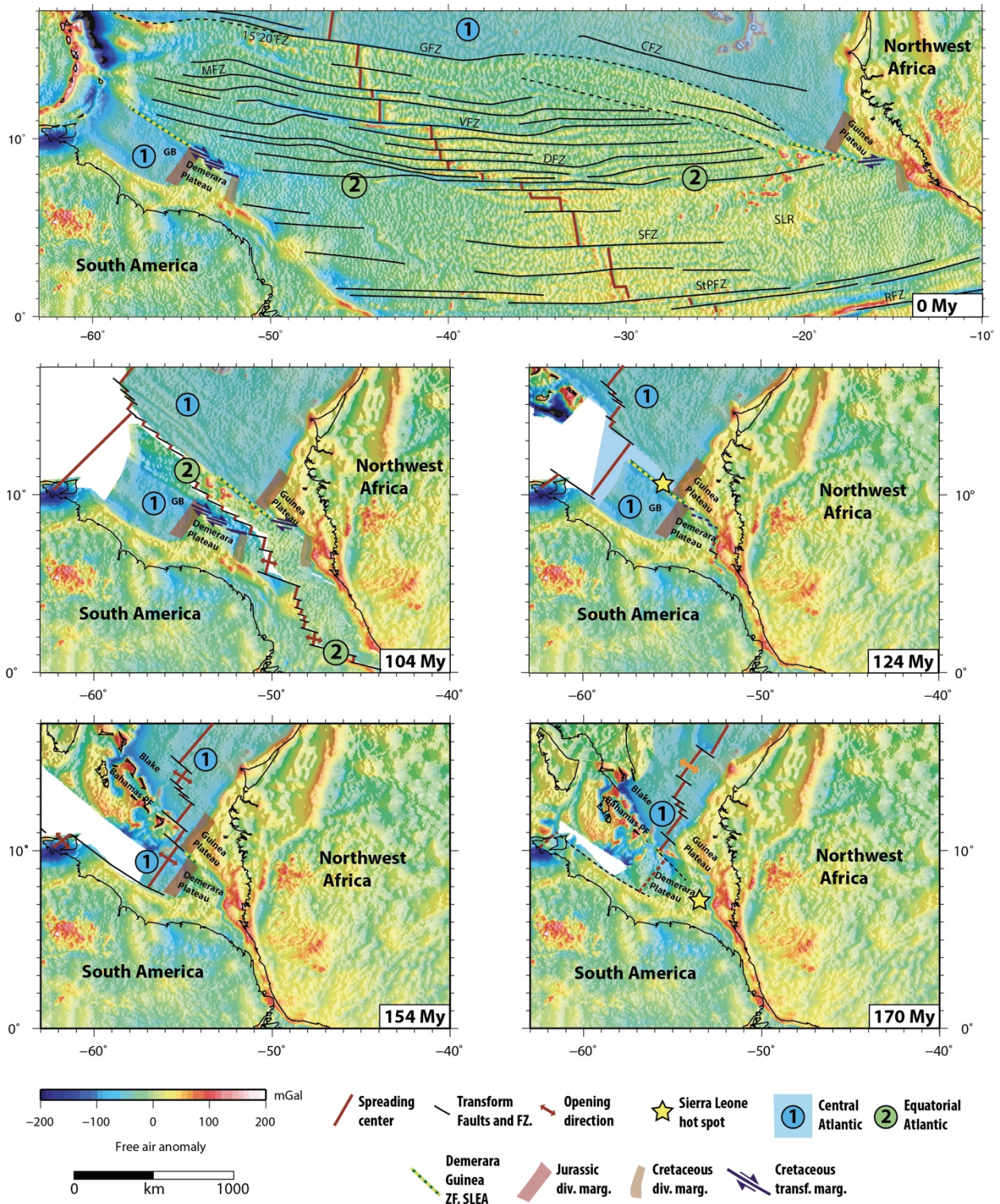
- 1040 Olyphant, J.R., Johnson, R.A., Hughes, A.N., 2017. Evolution of the Southern Guinea Plateau: implications on
1041 Guinea-Demerara Plateau formation using insights from seismic, subsidence, and gravity data.
1042 *Tectonophysics* 717, 358–371.
- 1043 O'Reilly, B., Hauser, F., Ravaut, C., Shannon, P., Readman, P., 2006. Crustal thinning, mantle exhumation and
1044 serpentinization in the Porcupine Basin, offshore Ireland: evidence from wide-angle seismic data. *J.*
1045 *Geol. Soc.* 163, 775–787. [https://doi.org/ 10.1144/0016-76492005-079](https://doi.org/10.1144/0016-76492005-079).
- 1046 Parsieglä, N., Gohl, K., Uenzelmann-Neben, G., 2007. Deep crustal structure of the sheared South African
1047 continental margin: first results of the Agulhas-Karoo Geoscience Transect. *S. Afr. J. Geol.* 110 (2–3),
1048 393–406.
- 1049 Paton, D., Pindell, J., McDermott, K., Bellingham, P., Horn, B., 2017. Evolution of seaward-dipping reflectors
1050 at the onset of oceanic crust formation at volcanic passive margins: insights from the South Atlantic.
1051 *Geology* 45. <https://doi.org/10.1130/G38706.1>.
- 1052 Pattier, F., Loncke, L., Gaullier, V., Basile, C., Maillard, A., Imbert, P. and Loubrieu, B., 2013. Mass-transport
1053 deposits and fluid venting in a transform margin setting, the eastern Demerara Plateau (French
1054 Guiana). *Marine and Petroleum Geology*, 46, 287–303.
- 1055 Pattier, F., Loncke, L., Imbert, P., Gaullier, V., Basile, C., Maillard, A., Roest, W.R., Patriat, M., Vendeville, B.C.,
1056 Marsset, T., 2015. Origin of an enigmatic regional Mio-Pliocene unconformity on the Demerara
1057 Plateau. *Marine Geology* 365, 21–35.
- 1058 Pindell, J.L., Kennan, L., 2009. Tectonic evolution of the Gulf of Mexico, Caribbean and northern South
1059 America in the mantle reference frame: an update. Geological Society, London, Special Publications
1060 328, 1–55.
- 1061 Planert, L., Behrmann, J., Jokat, W., Fromm, T., Ryberg, T., Weber, M., Haberland, C., 2017. The wide-angle
1062 seismic image of a complex rifted margin, offshore North Namibia: implications for the tectonics of
1063 continental breakup. *Tectonophysics* 716, 130–148.
- 1064 Planke, S., Eldholm, O., 1994. Seismic response and construction of seaward dipping wedges of flood basalts:
1065 Vøring volcanic margin. *Journal of Geophysical Research: Solid Earth* 99(B5), 9263–9278.
- 1066 Rabinowitz, P.D. & La Brecque, J., 1979. The Mesozoic South Atlantic Ocean and evolution of its continental
1067 margins, *Journal of Geophysical Research* 84(B11), 5973–6001.
- 1068 Reston, T.J., 2009. The structure, evolution and symmetry of the magma-poor rifted margins of the North and
1069 Central Atlantic: A synthesis. *Tectonophysics* 468 (1–4), 6–27.
- 1070 Reuber K., Pindell J., Horn B., 2016. Demerara Rise, offshore Suriname: Magma-rich segment of the Central
1071 Atlantic Ocean, and conjugate to the Bahamas hotspot. *Interpretation*, 4(2), T141-T155. doi:
1072 10.1190/INT-2014-0246.1
- 1073 Sandwell, D. T., & Smith, W. H., 2009. Global marine gravity from retracked Geosat and ERS-1 altimetry:
1074 Ridge segmentation versus spreading rate. *Journal of Geophysical Research: Solid Earth*,
1075 114(B1). Sapin, F., Davaux, M., Dall'Asta, M., Lahmi, M., Baudot, G., Ringenbach, J.-C., 2016. Post-rift
1076 subsidence of the French Guiana hyper-oblique margin: from rift-inherited subsidence to Amazon
1077 deposition effect. Geological Society, London, Special Publications 431, 125–144.
- 1078 Sapin, F., Davaux, M., Dall'Asta, M., Lahmi, M., Baudot, G., Ringenbach, J.C., 2016. Post- rift subsidence of the
1079 French Guiana hyper-oblique margin: from rift-inherited subsidence to Amazon deposition effect.
1080 *Geol. Soc. Lond., Spec. Publ.* 431 (1), 125–144.
- 1081 Sayers, B., Cooke, R., 2018. The MSGBC Basin, *Geoexpro*, Vol. 15, No. 5.
- 1082 Schimschal, C.M., Jokat, W., 2018. The crustal structure of the continental margin east of the Falkland Islands.
1083 *Tectonophysics* 724-725, 234–253. <https://doi.org/10.1016/j.tecto.2017.11.034>.
- 1084 Schimschal, C.M., Jokat, W., 2019. The crustal structure of the Maurice Ewing Bank. *Tectonophysics* 769,
1085 228190.
- 1086 Schön, J.H., 1996. *Physical Properties of Rocks: Fundamentals and Principles of Petrophysics*, vol. 18.
1087 *Handbook of Geophysical Exploration. Seismic Exploration.*
- 1088 Sheridan, R. E., Houtz, R. E., Drake, C. L., and Ewing, M., 1969. Structure of continental margin off Sierra
1089 Leone, West Africa; *Journal of Geophysical Research*, 74(10), 2512-2530.
- 1090 Stica, J. M., Zalán, P. V., & Ferrari, A. L., 2014. The evolution of rifting on the volcanic margin of the Pelotas
1091 Basin and the contextualization of the Paraná–Etendeka LIP in the separation of Gondwana in the
1092 South Atlantic. *Marine and Petroleum Geology*, 50, 1-21.
- 1093 Tallobre, C., Loncke, L., Bassetti, M. A., Giresse, P., Bayon, G., Buscail, R., Sotin, C., 2016. Description of a
1094 contourite depositional system on the Demerara Plateau: Results from geophysical data and
1095 sediment cores. *Marine Geology*, 378, 56-73.
- 1096 Villeneuve, M., & Cornée, J. J., 1994. Structure, evolution and palaeogeography of the West African craton
1097 and bordering belts during the Neoproterozoic. *Precambrian Research*, 69(1-4), 307-326.

- 1098 Vogt, U., Makris, J., O'Reilly, B.M., Hauser, F., Readman, P.W., Jacob, A.B., Shannon, P. M., 1998. The Hatton
1099 Basin and continental margin: crustal structure from wide- angle seismic and gravity data. *J. Geophys.*
1100 *Res. Solid Earth* 103 (B6), 12545–12566.
- 1101 Wade, J.A, MacLean, B.C., 1990. The Geology of the southeastern margin of Canada, M.J Keen, C.A Williams
1102 (Eds.), *Geology of Canada, Geology of the Continental Margin of Eastern Canada*, Geological Survey of
1103 Canada (1990), pp. 167-238
- 1104 Welford, J.K., Shannon, P.M., O'Reilly, B.M., Hall, J., 2012. Comparison of lithosphere structure across the
1105 Orphan Basin–Flemish Cap and Irish Atlantic conjugate continental margins from constrained 3D
1106 gravity inversions. *J. Geol. Soc.* 169 (4), 405–420.
- 1107 Wessel, P., & Smith, W. H., 1991. Free software helps map and display data. *Eos, Transactions American*
1108 *Geophysical Union*, 72(41), 441-446.
- 1109 White, R.S., Smith, L.K., 2009. Crustal structure of the Hatton and the conjugate East Greenland rifted
1110 volcanic continental margins, NE Atlantic. *J. Geophys. Res. Solid Earth* 114 (B2).
- 1111 White, R.S., McKenzie, D., O'Nions, R.K., 1992. Oceanic crustal thickness from seismic measurements and
1112 rare earth element inversions. *J. Geophys. Res.* 97 (B13), 19683–19715.
1113 <https://doi.org/10.1029/92JB01749>.
- 1114 White, R.S., Smith, L.K., Roberts, A.W., Christie, P.A.F., Kusznir, N.J., 2008. Lower- crustal intrusion on the
1115 North Atlantic continental margin. *Nature* 452 (7186), 460.
- 1116 Zelt, C. A., & Smith, R. B., 1992. Seismic travelttime inversion for 2-D crustal velocity structure. *Geophysical*
1117 *journal international*, 108(1), 16-34.
- 1118 Zinecker, M. P. (2020). Structural and Stratigraphic evolution of three Mesozoic, rifted passive margins:
1119 Guinea Plateau, Demerara Rise and Southern Gulf of Mexico. PhD Thesis. Univ. of Houston (302 pp).
- 1120

1121 **List of figures**

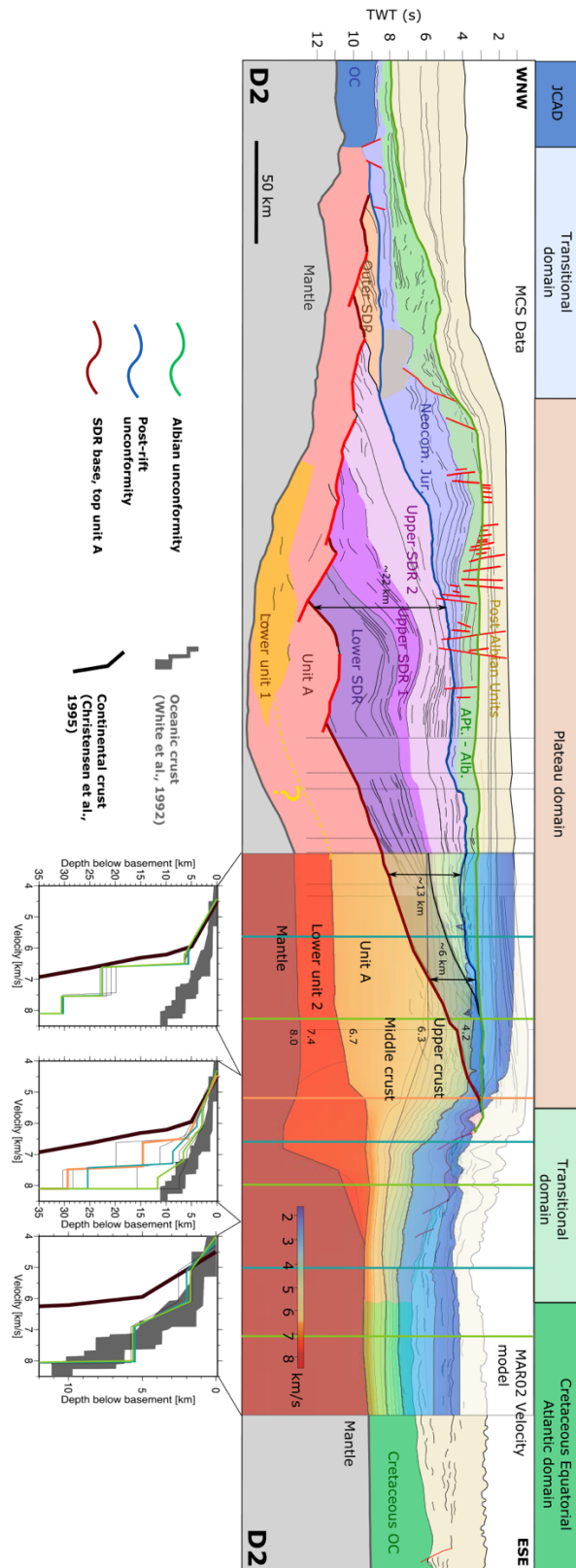


1122
 1123 **Figure 1:** Bathymetric (depths in meters) maps of the Demerara A) and Guinea B) conjugated
 1124 Transform Marginal Plateaus. Location of the presented synthetic line drawings from the
 1125 Guinea TMP: G1 to G3, and from the Demerara TMP: D1 to D7. Location of velocity models from
 1126 the MARGATS experiment MAR01 and MAR02 in red; GB: Guyana Basin; SLNEA: Southern
 1127 Limit of the Northern Equatorial Atlantic, GFZ: Guinea Fracture Zone.

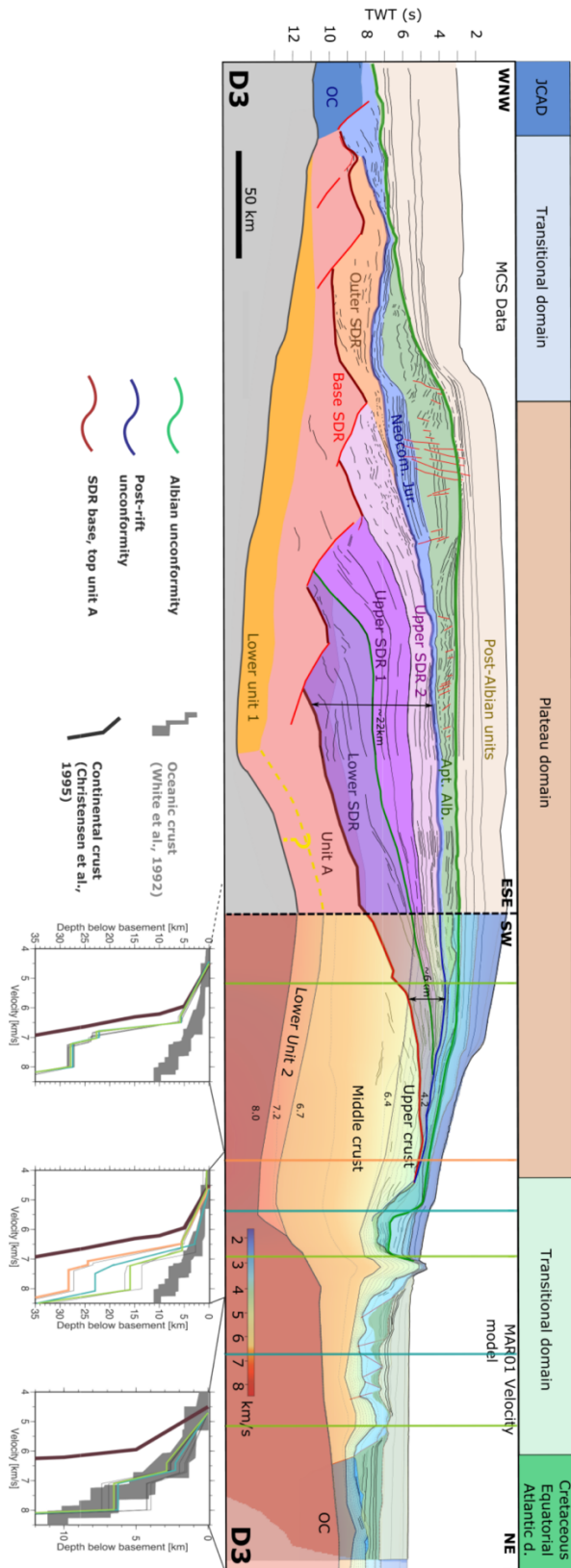


1128
1129
1130
1131
1132
1133
1134
1135
1136
1137

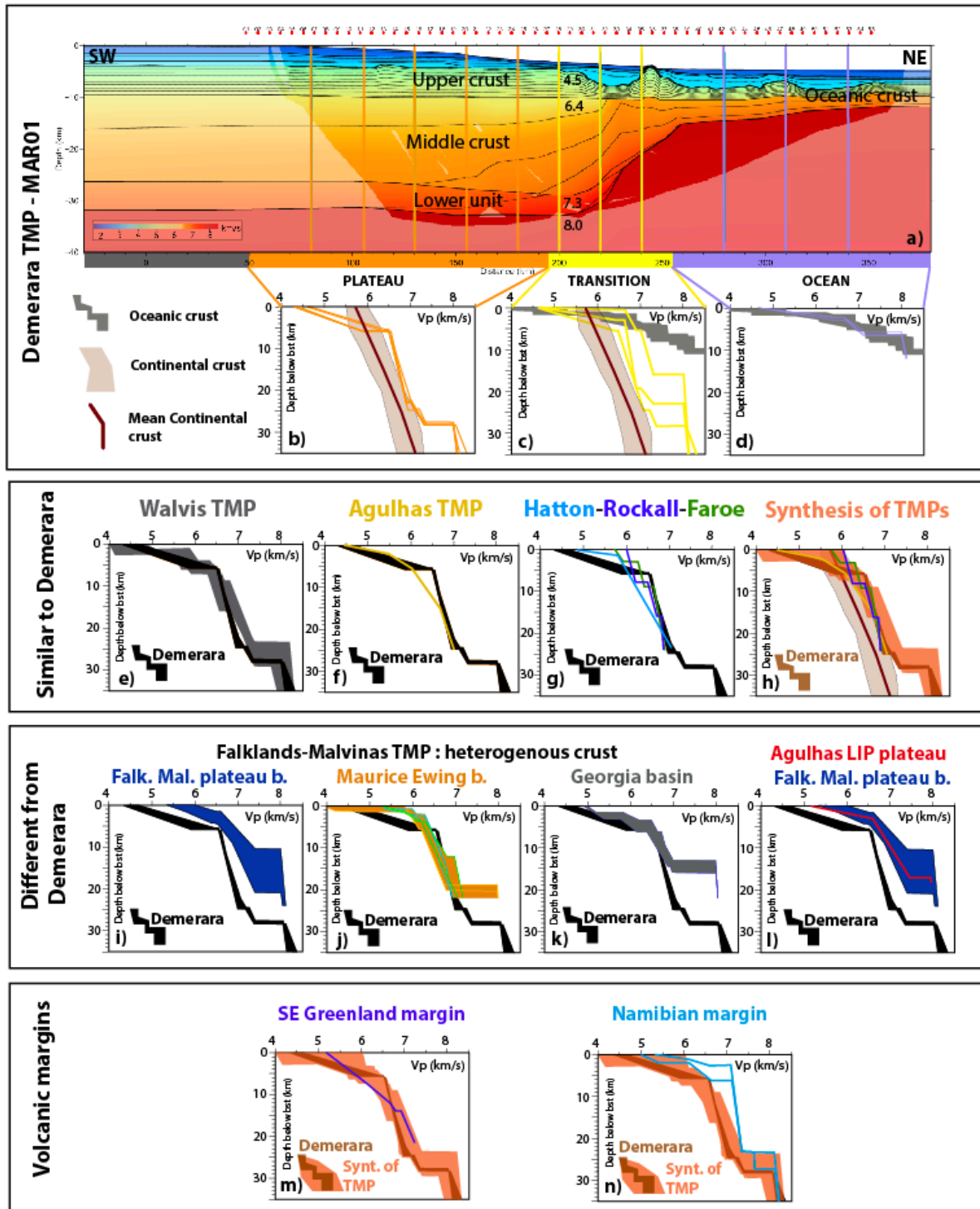
Figure 2: Location of Demerara and Guinea TMPs at the present (0 My); Maps represent the free air gravity anomaly (Sandwell and Smith, 2009); Central and Equatorial Atlantic are labeled respectively in blue and green; FZ: Fracture Zone, GFZ: Guinea FZ, CFZ: Cap Vert FZ, MFZ: Marathon FZ, VFZ: Vema FZ, DFZ: Doldrums FZ, SFZ: Strakhov FZ, StPFZ: Saint Paul FZ, RFZ: Romanche FZ, 15°20'FZ, SLR: Sierra Leone Rise; Kinematic reconstructions at 104, 124, 154 and 170 My, performed with GPlates using rotation poles from earlier studies (Campan, 1995; Moulin et al., 2010); positions of Sierra Leone hot spot is from Basile et al. (2020); GB: Guyana Basin.



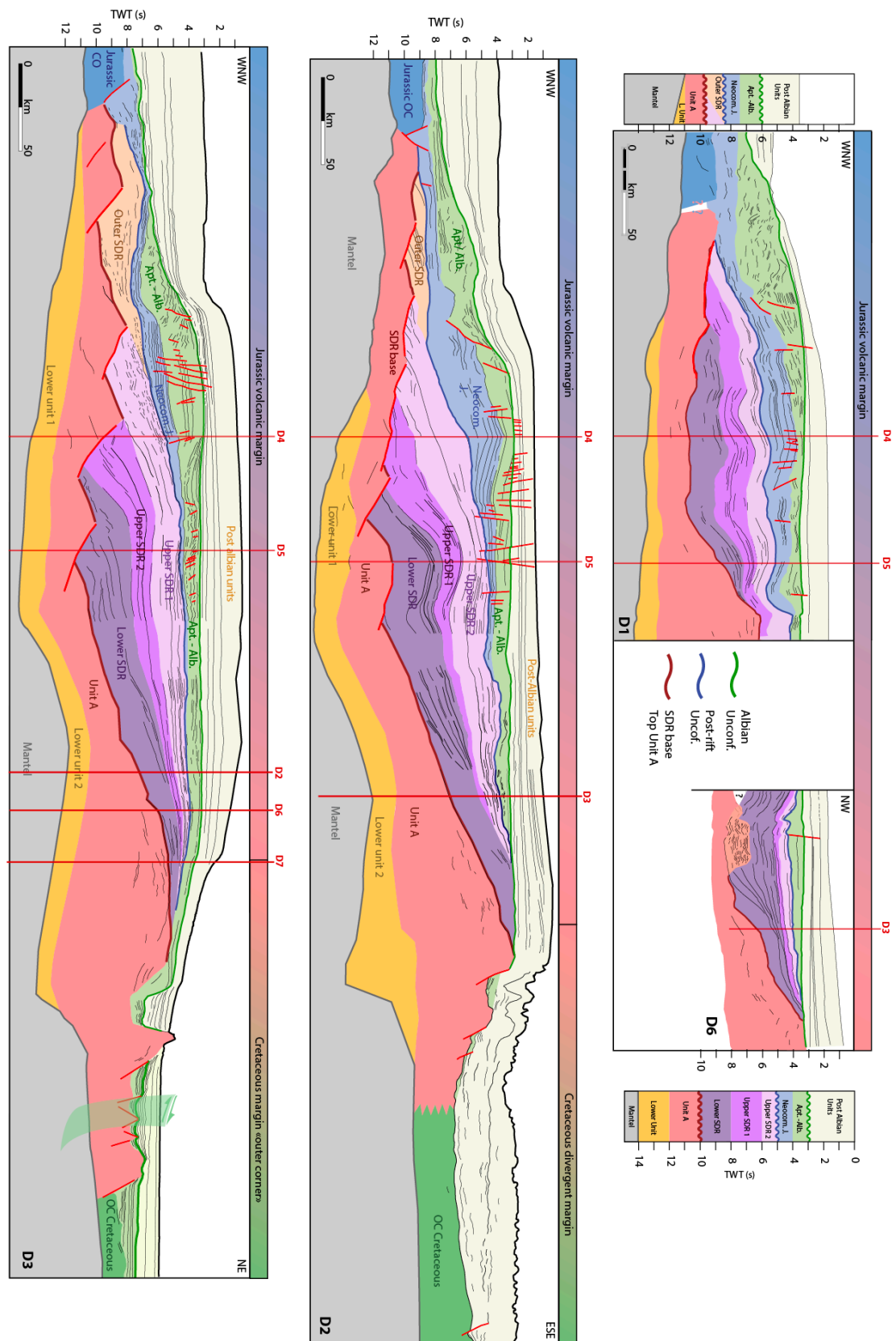
1138
 1139 **Figure 3:** Composite line D2 through the Demerara Plateau (see figure 1 for location), composed of
 1140 MCS data in the west and combined wide-angle (MAR02) and MCS data in the east; detailed
 1141 comparison of V_z profile within different domains with V_z “standard” of continental and
 1142 oceanic crusts (Christensen and Mooney, 1995; White et al., 1992), modified after Museur et
 1143 al., 2021.
 1144



1145
 1146 **Figure 4:** Composite line D3 through the Demerara Plateau (see figure 1 for location) composed of
 1147 MCS data in the west and combined wide-angle (MAR01) and MCS data to the north-east;
 1148 detailed comparison of Vz profile within different domains with Vz “standard” of continental
 1149 and oceanic crusts (Christensen and Mooney, 1995; White et al., 1992), modified after Museur
 1150 et al. (2021).

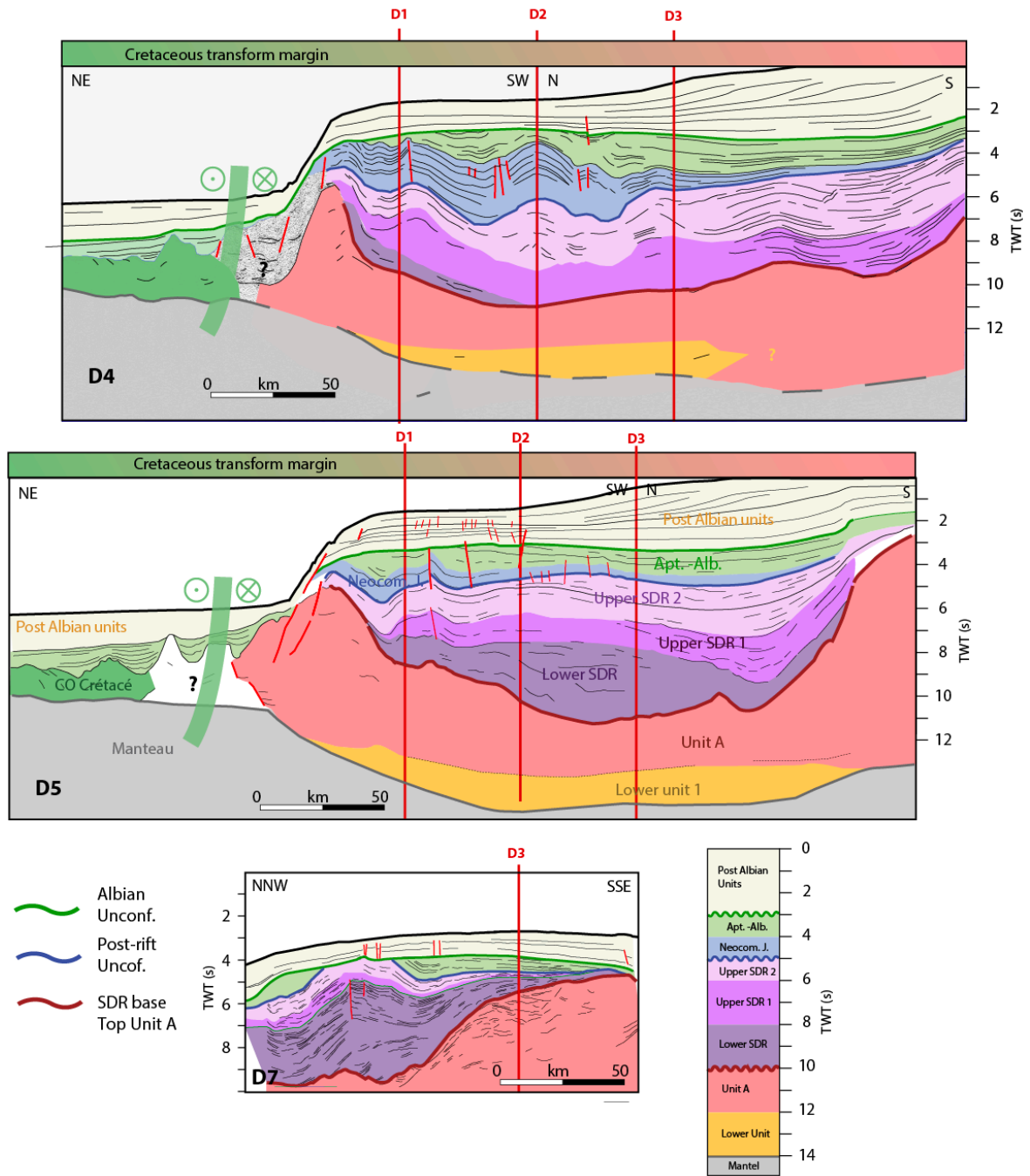


1151
 1152 **Figure 5:** a) velocity model MAR01 see *Museur et al. (2021)* for details; b), c) and d) *V_z* comparison
 1153 between different domains of the Demerara Plateau and continental and oceanic crusts
 1154 (*Christensen and Mooney, 1995; White et al., 1992*); e), f) and g) *V_z* comparisons with other
 1155 TMPs similar to the Demerara Plateau: the Walvis Ridge (*Planert et al., 2017*), the Agulhas
 1156 TMP (*Parsieglä et al., 2007*), the Faroe Bank (*Funck et al., 2008*), the Hatton Bank (*White and*
 1157 *Smith, 2009*), the Rockall Bank (*Vogt et al., 1998*); h) *V_z* synthesis of TMPs; i), j), k) and l) *V_z*
 1158 comparisons with other TMPs different from the Demerara Plateau: the Falklands-Malvinas
 1159 Bank (*Schimschal and Jokat, 2018; Schimschal and Jokat, 2019*), the Central Agulhas Plateau
 1160 (*Parsieglä et al., 2007*); m) and n) *V_z* comparisons with volcanic margins: the SE Greenland
 1161 margin (*Hopper et al., 2003*) and the Namibian margin (*Bauer et al., 2000*).



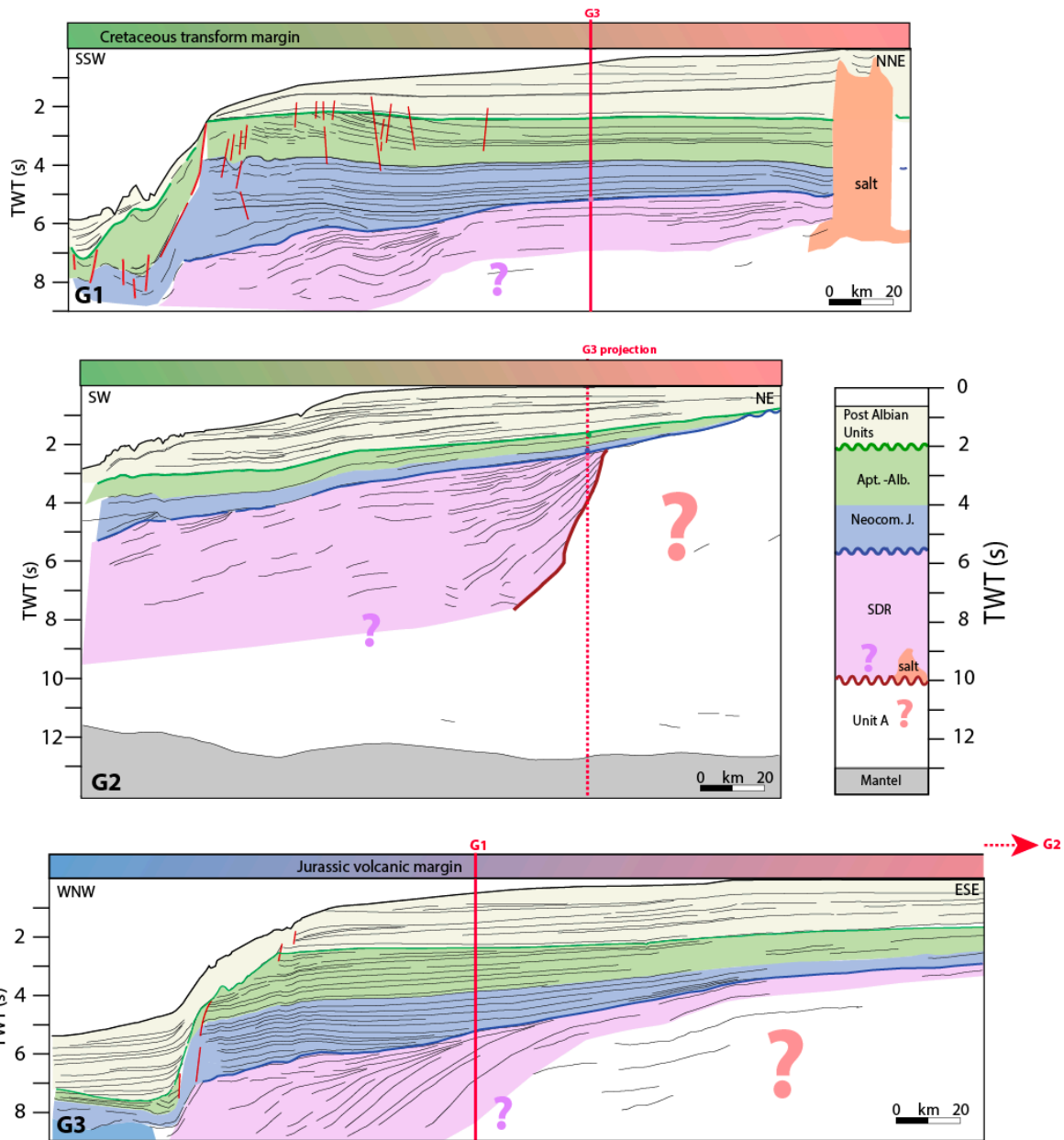
1162
 1163
 1164
 1165

Figure 6: Line drawings and interpretations of composite Demerara Plateau lines D1, D2, D3 and D6 (see figure 1 for location). D2 and D3 are obtained from interpretation of sub-coincident MCS and wide-angle data.



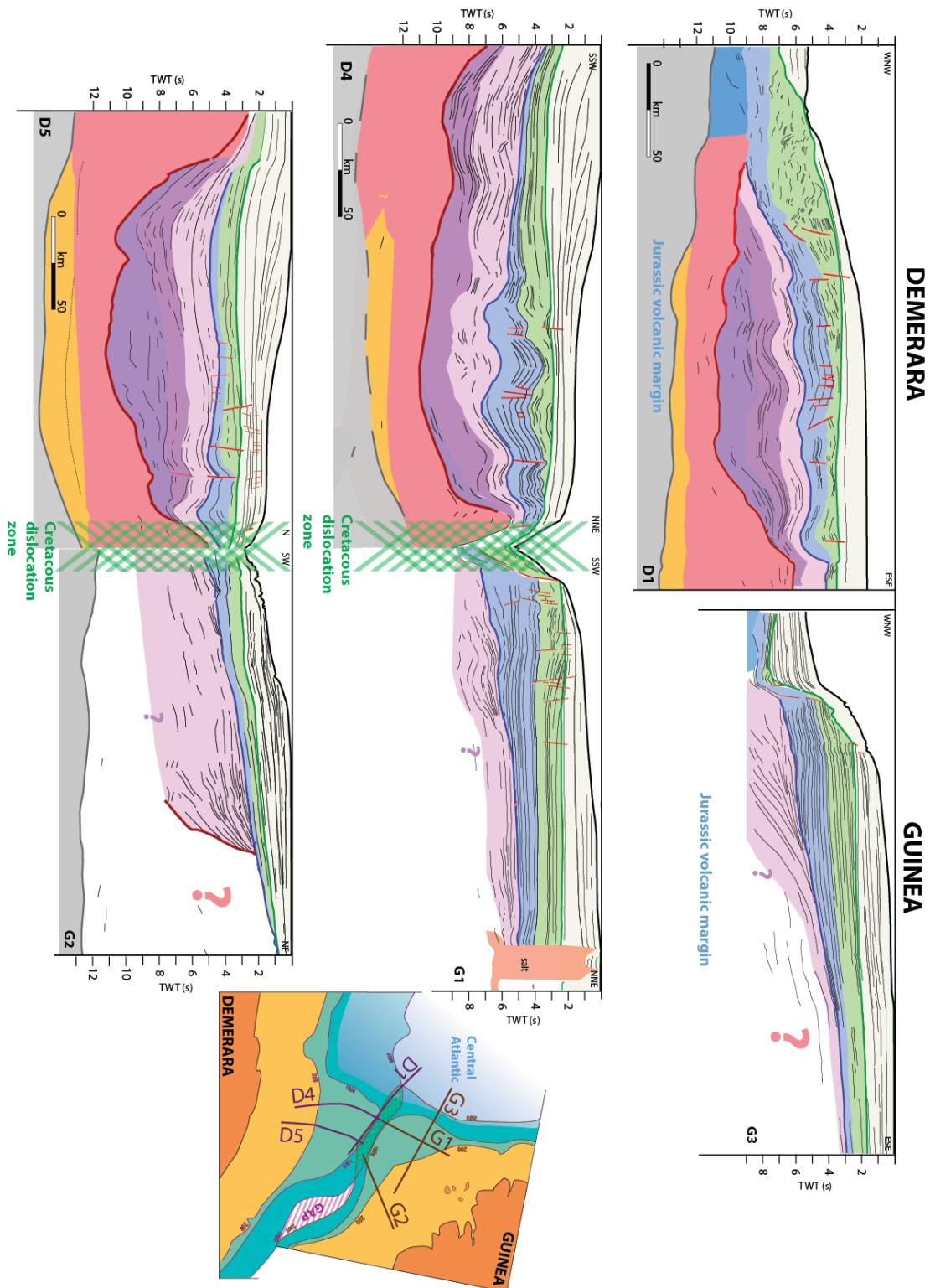
1166
1167
1168

Figure 7: Line drawings and interpretations of Demerara Plateau composite lines D4, D5 and D7 (see figure 1 for location).

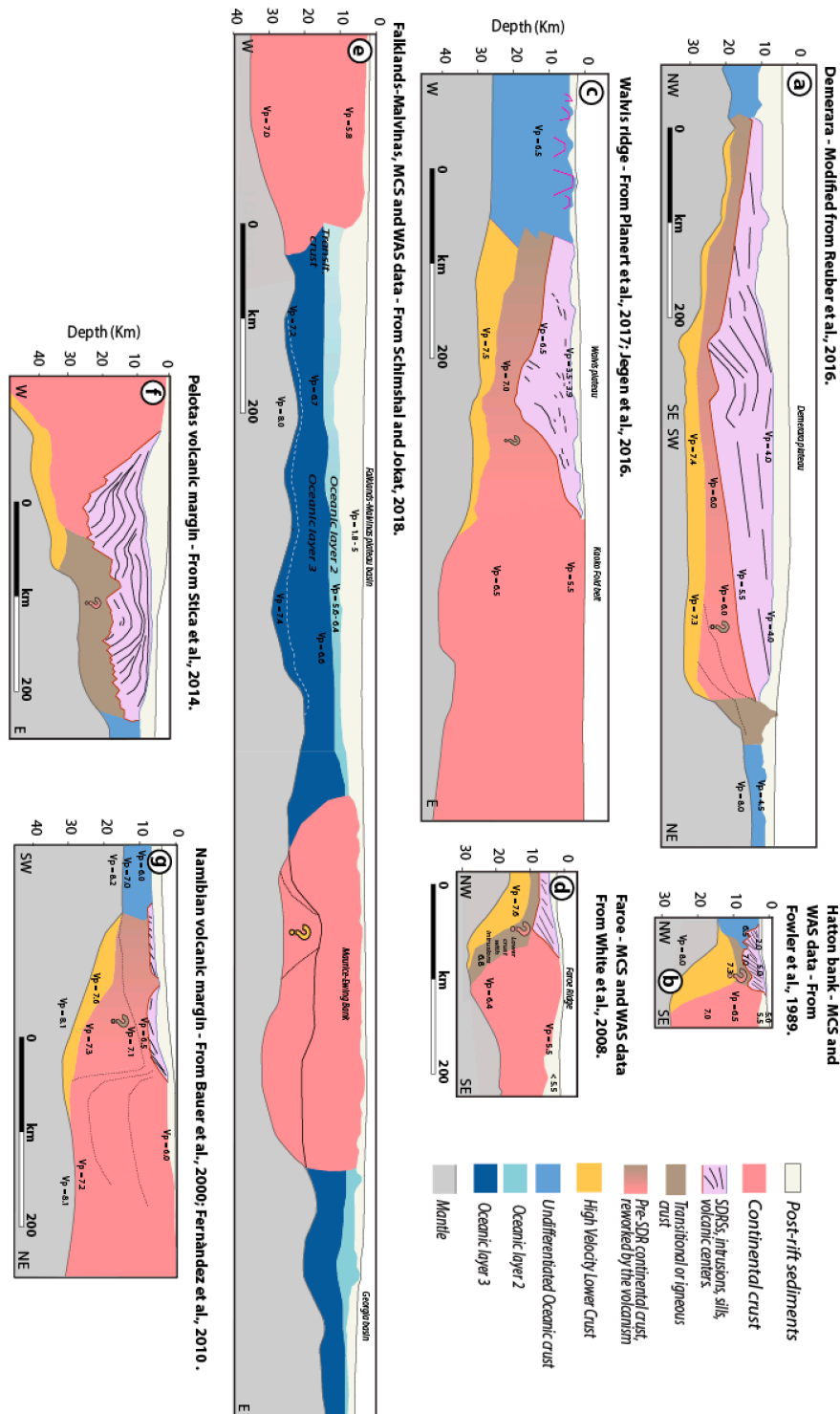


1169
1170
1171

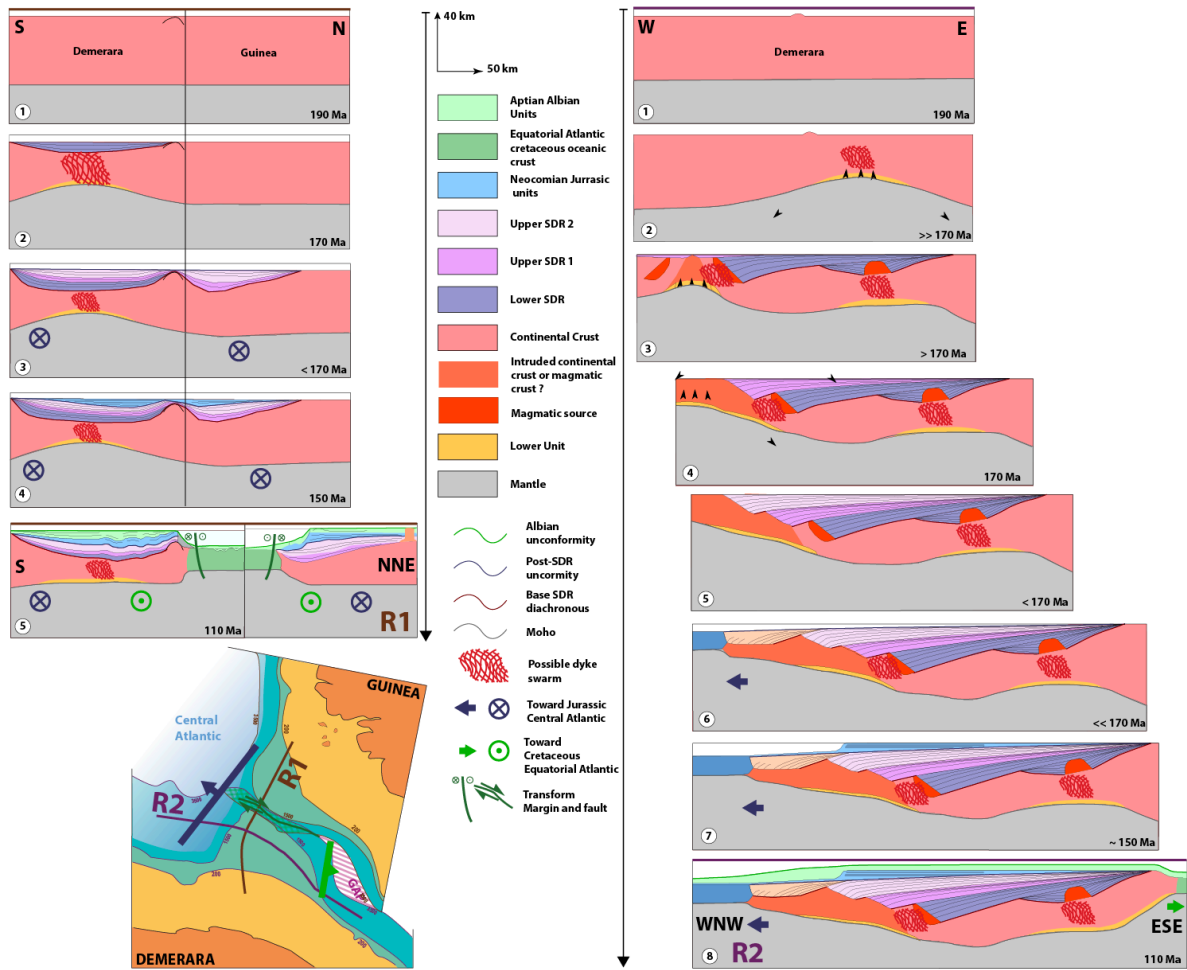
Figure 8: Line drawings and interpretations of Guinea Plateau lines G1, G2 and G3 (see figure 1 for location).



1172
 1173 **Figure 9:** Comparison of WNW-ENE sections of Demerara (D1) and Guinea (G3) TYPs shown in the
 1174 same scale across the Jurassic volcanic margin. Inset shows our hand-made morphological
 1175 reconstruction based on Moulin et al. (2010) and Mercier de Lépinay (2016) works, made for
 1176 a time period of 125 My. Lowermost two profiles represent our attempt to put line drawings
 1177 of sections D4 and D5 from the Demerara TYP and G1 and G2 for the Guinea TYP face to face
 1178 at the same scale.



1179
 1180 **Figure 10:** Comparison between crustal structures of : a) the Demerara Plateau (Modified from
 1181 Reuber et al., 2016 and Museur et al., 2021); b) the Hatton Bank (Fowler et al., 1989); c) the
 1182 Walvis Ridge (From Planert et al., 2017; Jegen et al., 2016); d) the Faroe Bank (White et al.,
 1183 2008); e) the Falklands-Malvinas TMP (Schimschal and Jokat, 2018, 2019); f) the Pelotas
 1184 Volcanic Margin (Stica et al., 2014); g) the Namibian Volcanic Margin (Bauer et al., 2000;
 1185 Fernandez et al., 2010); After Museur et al., 2021.



1186
 1187
 1188
 1189
 1190
 1191

Figure 11: Left: schematic evolution of both conjugated plateaus from a north-south point of view (R1); Right: schematic evolution of the Demerara Plateau from a west-east point of view (R2); Lower-left hand-made morphological reconstruction based on Moulin et al. (2010) and Mercier de Lépinay (2016), probably around 125 My (see also Figure 2).